Elucidation of mechanism that determines *N*-linked sugar chain pattern expressed in cells or tissues using cDNA macroarray and 2 dimensional HPLC analyses

Akihiro Ishii

Doctor of Philosophy

Department of Physiological Sciences, School of Life Science,
The Graduate University for Advanced Studies
and
Division of Neurobiology and Bioinformatics,
National Institute for Physiological Sciences, Okazaki National Research Institutes

2003

Table of Contents

Abstract

N-linked sugar chains on glycoproteins are indispensable for the normal development. The expression of *N*-linked sugar chains is strictly regulated spatially and temporally, and tissue specific expression patterns of *N*-glycans are observed. Comparison of the mouse brain as well as the human brain revealed little variation among individuals of each species. However, molecular mechanisms that are responsible for the strict regulation of the *N*-linked sugar chains remain largely unknown. The expression of the *N*-glycans is based on the orchestrated action of many enzymes, glycosyltransferases and glycosidases, which catalyze biosynthesis and degradation of glycochains. The expression patterns of genes that encode these enzymes are, therefore, necessary to understand the regulatory mechanisms of *N*-glycan biosynthesis. In the present study, I developed a cDNA macroarray, with which expression of most of the glycosyltransferase and glycosidase genes can be analyzed at the same time. I chose this sensitive system because the expression levels of these genes were mostly too low to be analyzed by a microarray system. Using the cDNA macroarray system, I analyzed the gene expression patterns of more than 110 glycosyltransferases and glycosidases in the brain from 12-day mouse embryos, and in the brain, kidney, and liver from 12-week adult mice, and correlated them with the expression patterns of *N*-linked sugar chains in these tissues. The analyses revealed the tissue specific expression patterns of the glycosyltransferase and glycosidase genes as well as tissue specific *N*-glycan expression profiles. For example, whereas Golgi-mannosidase IB and polypeptide GalNAc Transferase I genes were equally expressed in these four tissues, α2, 8-sialyltransferase V and β1, 4-galactosyltransferase VI genes were highly

expressed in the postnatal 12-week brain. mRNA amounts of some of the genes, which were differentially expressed in the four tissues were further verified by means of RT-PCR analyses. By comparing the gene expression and *N*-glycan expression profiles, I could obtain several new findings; bisecting structures were exclusively catalyzed by *N*-acetylglucosaminyltransferase III, and a core fucose is exclusively synthesized by fucosyltransferase VIII. In this study, I also compared the expression of the glyco-genes and *N*-linked sugar chains, and identified correlation between gene expression and *N*-linked sugar chains. For example, the gene expression of glucosidase I, glucosidase II and ER-mannosidase I was highly correlated Golgi-mannosidase IB with correlation coefficients (0.82, 0.74 and 0.80, respectively). Such coordinated expression could be necessary and important physiologically to biosynthesize the *N*-linked sugar chains smoothly and efficiently. cDNA macroarray system as well as high-throughput *N*-glycan analyzing system will provide significant information for the elucidation of the regulatory mechanisms and biological function of the *N*-linked sugar chains.

Abbreviations

The nomenclature of oligosaccharide structures is as follows: An (where n = 0-2) indicates the number of antennae linked to the trimannosyl core (M3B); Gn (where n = 0-4), the number of galactose residues attached via β1–4 linkage to non-reducing ends; G'n (where n = 1-2), the number of galactose residues attached via β1–3 linkage to the non-reducing ends; F, with core fucosylation; Fo, with outer arm fucosylation attached via β1-3 linkage to *N*-acetylglucosamine residues; B, with bisecting *N*-acetylglucosamine residues.

12W:	12 weeks
E12:	embryonic day 12
ER:	endoplasmic reticulum
EXT:	hereditary multiple exostoses
EXTL:	multiple exostoses-like
Fuc-T:	fucosyltrnsferase
GAPDH:	glyceraldehyde-3-phosphate dehydrogenase
GAL3ST:	galactosylceramide 3-sulfotransferase

GalNAcT:	*N*-acetylgalactosaminyltransferase
GnT:	*N*-acetylgucosaminyltransferase
GPA:	GlcNAc phosphodiester α acetylglucosaminidase
GT:	galactosyltransferase
GU:	glucose unit
HGPT:	hypoxanthine guanine phosphoribosyltransferase
HS2ST:	heparan sulfate 2-sulfotransferase
HS3ST:	D-glucosaminyl 3-O-sulfotransferase
HS6ST:	D-glucosaminyl 6-O-sulfotransferase
HPLC:	high performance liquid chromatography
MT:	mannosyltransferase
MU:	mannose unit
NDST:	heparan sulfate *N*-deacetylase/*N*-sulfotransferase
PA-:	pyridylamino
PCR:	polymerase chain reaction
PLP:	proteolipid protein

RA:	relative abundance
RT-PCR:	reverse transcriptase-PCR
SSEA-1	stage specific embryonic antigen-1
ST:	sialyltransferase
ST8Sia:	α-2, 8-sialytransferase
ST3Gal:	Gal α-2, 3-sialytransferase
ST6Gal:	Gal α-2, 6-sialytransferase
ST6GalNAc:	GalNAc α-2, 6-sialyltransferase
XT:	xylosyltransferase

Introduction

N-linked sugar chains are associated with most proteins found on the mammalian cell surface and in secretions. *N*-linked glycosylation is essential for the folding, intracellular transport, function, stability and secretion of glycoproteins (Helenius et al., 2001). *N*-linked sugar chains on cell surface glycoproteins are suggested to be involved in various cellular functions including cell-cell and cell matrix interactions. In the developing nervous system, these molecules are supposed to play important roles in specific events such as cell adhesion, differentiation, synaptogenesis, and myelinogenesis.

Glycosylation of membrane and secretory glycoproteins comprises a cascade of steps that implicate a number of glycosidases and glycosyltransferases, and commences in the lumen of the endoplasmic reticulum (ER) concomitant with protein translation and translocation (Jenkins et al., 1996; Geetha-Habib et al., 1988; Kornfeld et al., 1985). This initial glycosylation event, known as *N*-linked core glycosylation, involves the transfer of Glc3Man9GlcNAc2 unit to acceptor asparagine residues in the tripeptide sequon Asn-Xaa-Ser/Thr and is catalyzed by the enzyme oligosaccharyltransferase (Jenkins et al., 1996; Geetha-Habib et al., 1988; Kornfeld et al., 1985). Upon arrival to the *cis*-Golgi network, the initial mannose-rich core chains are trimmed by mannosidases I and II of the *cis*-Golgi. In the *medial* and *trans*-Golgi formation of complex type of glycans ensues and is terminated by the addition of sialic acid in the *trans*-Golgi network (TGN) (Jenkins et al., 1996; Geetha-Habib et al., 1988; Kornfeld et al., 1985; Spiro et al., 1991; Orlean et al., 1992). In the past decade, a number of glycosidases and glycosyltransferases were purifed and examined for their biological properties, which suggested that there are many kinds of glycosidases and

glycosyltransferase in various tissues.

Cloning of glycosyltransferases has revealed the existence of families of homologous glycosyltranferases with a similar catalytic activity but encoded by different genes. In a cell, more than 130 glycosyltransferases genes were cloned. Thus, many steps in the pathways of *N*-glycosylation appear to be catalyzed by several related glycosyltransferases that may show slight differences in properties and substrate specificities. The expression levels of these enzymes are cell type specific and appear to be strictly regulated during the growth and differentiation of cells, and during tissue development. The enzyme expression profiles are known to be altered in many pathological conditions.

During a course of the development and regeneration of the central nervous system (CNS), glycosylation on the cell surface have been examined by using lectin, and / or anti-carbohydrate antibodies (Allendoerfer et al., 1999; Ronn et al., 2000). For example, a LewisX antigen, was examined by anti-CD15/SSEA-1 antibody to reveal that it is spatiotemporally regulated in the CNS during development. The regulated expression of glyco-antigens suggested that the carbohydrates on the cell surface play important roles in the neural tissue formation. The relatively simple and straightforward methods of histochemical characterization of glycoproteins are well-suited, although there are several limitations, for sugar chain analysis. (i) These methods require antigen-specific lectin or anti-carbohydrate antibody, which limited number of sugar chain structures ready for analysis though there are no antibody or lectins that recognize the whole structure of sugar chain specifically. (ii) Since lectins and anti-carbohydrate antibodies usually recognize terminal structures of glyco-antigen (glycoproteins as well as glycolipids), these histochemical methods provide little

information on the whole structure of sugar chains. (iii) The histochemical approach is generally inadequate for quantitative or fine structural analyses.

An alternative method to analyze *N*-linked sugar chains has been developed recently, using high-performance liquid chromatography after hydrazinolysis and pyridylamination. This method can analyze not only the epitopes but the entire structure of sugar chains expressed in tissues. Previously, complete characterizations of neutral and sialylated *N*-linked sugar chains expressed in adult rat brains have been performed systematically (Chen et al., 1998, Zamze et al., 1998). Furthermore, it has been shown that the profiles of their expressions are highly conserved in the brain from adult human, mouse and rat (Albach et al., 2001). However, the methods used by Albach et al. and Zamze et al. required many chromatographic steps for separation and purification of each sugar chain, making it unsuitable for analyzing a large number of samples or small amounts of samples. Later the research group of Hase (Hase et al., 1981; 1987; 1988) and Ikenaka (Fujimoto et al., 1999; Otake et al., 2001) developed a system with which one could determine relative amount of *N*-linked sugar chains expressed in whole tissues easily and reproducibly from amounts as low as 2 mg of acetone precipitated brain tissue (Fujimoto et al., 1999). In this study, I applied this method to the analysis of *N*-linked sugar chains from various mouse tissues and cell lines.

In a previous study, Ikeda revealed that (i) the expression pattern of the *N*-linked sugar chains changes dramatically during developmental stages of the mouse brain, (ii) the expression pattern of *N*-linked sugar chains are well conserved among individuals (Ikeda, 2003). Based on these results, they suggested that the expression patterns of *N*-linked sugar chains are strictly regulated in a spatiotemporal manner.

However, molecular mechanisms that are responsible for the strict regulation of the *N*-linked sugar chains have not been elucidated yet.

To elucidate the regulatory mechanisms by comparing gene expression and sugar chain structures expressed on the cell surface, I developed a cDNA macroarray system as the first step. Then I analyzed the relative amounts of *N*-linked sugar chains and gene expression of the same sample and examined the correlation between their gene expression and *N*-linked sugar chains.

Materials and methods

PA-sugar chains used as standard were purchased from Takara (Japan) or Seikagaku Corporation (Japan). Neuraminidase derived from *Arthrobacter ureafaciens* were provided by from Nacalai Tesque (Japan). Hybond N, mRNA purification kit, Quick Prep Micro mRNA purification kit, and [α -^{32}P]dCTP were purchased from Amersham Biosciences (Japan). Trizol, Superscript II RNase H_ Reverse Transcriptase and RNaseOUT recombinant RNase inhibitor were purchased from Invitrogen (Japan). dATP, dCTP, dTTP, dGTP and *Taq* polymerase were purchased from Promega (Japan).

Cell culture

All cell lines used in this study (Neuro2a, N1E115, NB41A, C8D30, C8D1A and C8S) were obtained from the American Type Culture Collection (ATCC). Neuro2a, N1E115, C8D30, C8D1A and C8S cells were cultured in Dulbecco's modified

Eagle's medium containing 10% fetal calf serum, and maintained at 37℃ in a humidified atmosphere containing 5% CO_2. NB41A cells were cultured in Dulbecco's modified Eagle's medium containing 15% hourse serum and 2.5% fetal calf serum, and maintained at 37℃ in a humidified atmosphere containing 10% CO_2. They were routinely passaged according to the Manufacturer's instructions (ATCC). The cells were harvested by scraping into ice-cold PBS(-) and pelletted by centrifugation at 3000 rpm for 10 min at 4℃. The cell pellets were used for the analysis of *N*-linked sugar chains.

Array preparation

Cloning of Target DNA.

The sequences of target cDNA were retrieved from the Gene Bank database (National Center for Biotechnology Information). Polyadenylated mouse RNA, isolated from the 12-day embryonic brain, the liver, kidney and brain from 12-week adult mice were used to synthesize cDNA. The mRNA was reverse transcribed with oligo (dT_{17}) primers and Superscript II reverse transcriptase as per the manufacture’s

instruction. cDNA segments of 500-2500 bp long without repetitive or polyadenylated sequences were chosen for amplification by PCR reactions with primers that were synthesized and provided by Oligotechnomart (Japan). The PCR products were subcloned into pZErO-2 plasmid vector and their sequences were confirmed by direct sequencing method. Sequencing of the 5'-end of the cDNA insert was performed with M13 forward or reverse primer using a DYEnamic ET Terminator Cycle Sequencing kit and ABI377 sequencer (Applied Biosystems). To amplify cDNA inserts for arraying, the same PCR primers used for cDNA cloning were used. For each cDNA clone, 5 ng of the plasmid DNA was used as a template in 50 μl PCR reaction containing 10 mM Tris-HCl (pH 8.3), 50 mM KCl, 1.5 mM $MgCl_2$, 0.1% Triron X-100, 12.5μM of each primer, 0.2 mM dNTPs, and 3.25 units of *Taq* DNA polymerase. Amplification was done in a Peltier Thermal Cycler (MJ Research, Cambridge, MA) under the following conditions: initial denaturation at 95°C for 2 min; then 35 cycles of denaturation at 94°C for 30 s, annealing at 60°C for 30 s, and extension at 72°C for 1 min; and then a final extension at 72°C for 7 min. PCR products were precipitated with ethanol, then the precipitates were washed with 70% ethanol, and then the precipitates were dissolved in

TE buffer (10 mM Tris-HCl, 1 mM EDTA, pH 8.0) to be adjusted at 2 μg/μl. To examine the quality and quantity of the PCR products, they were run on 1.2% agarose gels (Nacalai). The PCR products were mixed with 2×Array-BPB (4 mM Tris-HCl, pH7.5, 0.4 mM EDTA, 24% (v/v) glycerol, 0.1% bromophenolblue) and transferred to a 384-well plate. The cDNAs were spotted onto the Hybond-N membranes (Amersham Bioscience) using a Microgrid II (BioRobotics). A 384 pin gridding head was used for spotting a grid of 384 blocks, each containing 4 spots for each sample, that is, each sample was spotted 4 times within a block. The spotted membranes were submerged in a denaturing solution (0.5 M NaOH, 1.5 M NaCl) and soaked for 1 min. The membranes were transferred into a neutralization solution (0.5 M Tris-HCl, pH 7.0, 1.5 M NaCl) soaked for 1 min, and then soaked in 2×SSC for 5 min. After drying, spotted PCR products on the membranes were cross-linked by ultraviolet light, and baked for 30 min under vacuum at 80℃ in a vacuum oven.

mRNA purification

Mice were perfused with PBS(-), then 12-day fetal brain and 12-week

postnatal brain, kidney and liver were extracted, then total RNA was extracted by Trizol reagent (Invitrogen). Poly (A) RNA was purified from total RNA by using mRNA purification kit according to the protocol (Amersham Pharmacia). The cell lines (Neuro2a, N1E115, NB41A, C8D1A, C8D30 and C8S) cells were rinsed quickly in ice-cold PBS, and mRNA was isolated by using Quick Prep Micro mRNA purification kit as per the manufacturer's instructions. The RNA concentration was quantitated by spectrophotometric analysis at 260 nm.

Probe Preparation

One μg of poly (A) RNA was mixed with 1.8 μg of random primers in a total volume of 3.25 μl, then heat denatured at 70℃ for 5 min, and then cooled on ice. Ten μl of [α -^{32}P] dCTP (3000 Ci/mmol), 1 μl of 0.1 M DTT, 5 μl of first-strand buffer (Invitrogen), 2 ml of dNTPs (10 mM each of dTTP, dGTP and dATP, and 37 μM dCTP), 20 U of RNASEOUT (Invitrogen), and 2 μl of Superscript II (invitrogen) were added to the sample mixture. Each sample was incubated at 42℃ for 1 h to synthesize ^{32}P-labeled cDNA. After one hour incubation, template RNA was degraded with 0.3 M

NaOH at 65°C for 30 min, and then the mixture was neutralized with 1 M Tris-HCl (pH 7.5). The ^{32}P-labeled cDNA was purified by Sepharose-G50 column to eliminate unincorporated ^{32}P-labeled nucleotides and very short synthetic cDNA. The cDNA sample was fractionated into 10 eluates, and the eluates with the highest radio-activity were pooled and used for hybridization.

Macroarray Hybridization and Data Analyses

Prehybridization of the cDNA macroarray membrane was done in prehybridization solution (5×SSPE, 50% (v/v) formamide, 5×Denhaldt's solution, 0.5% (v/v) SDS, 100 μg/ml hering sperm DNA) at 50°C for 4 h, and the membrane was rotated in 35×50 mm roller bottles. The purified probe was denatured in boiling water for 5 min, and then chilled on ice. Hybridization was performed by adding the denatured probe to the prehybridization solution, and incubated at 50°C for 20 h in a roller oven. The membranes were washed twice in 2×SSPE, 0.1% SDS for 10 min at room temperature, followed by two washings in 1×SSPE, 0.1% SDS at 65°C for 20

min. After a final wash with 0.1×SSPE, 0.1% SDS for 20 min at 65°C, the membranes were exposed to a Fuji BAS-MS2325 intensifying screen for 7 days at 4℃. Then the screen was scanned by a Fuji BAS 1800 II Phosphorimager (Fuji Photo Film Co., Ltd., Japan) at a maximum resolution of 50 μm. All the experiments were triplicated for each sample.

Pyridylamination of sugar chains released from tissue or cell samples

Tissues or cell pellets were homogenized with nine-fold volume of acetone using polytron homogenizer. After placing on ice for 1 hour, the homogenate was centrifuged at 2,150×g for 20 min. The pellet was dried in a Spinvac centrifuge. Acetone precipitated samples were manually hydrazynolyzed followed by *N*-acetylation, and pyridylaminated using the GlycoTag™.

Hydrazynolysis and N-acetylation

A lyophilized sample (2 mg) was heated with 200 μl anhydrous hydrazine at 100°C for 10 h. Excess hydrazine was evaporated *in vacuo*. The remaining trace of

hydrazine was removed by co-evaporation with toluene several times. The sugar chains released were *N*-acetylated with freshly prepared sodium bicarbonate solution (saturated, 200 μl) and acetic anhydride (8 μl) by incubation on ice. Five minutes later, another 200 μl of the bicarbonate solution and 8 μl of acetic anhydride were added. The reaction mixture was left to stand for 30 min on ice with occasional stirring. Dowex 50W-X2 (1 g, H^+ form, 100-200 mesh; Bio-Rad, Hercules, CA) was added to the solution to bring the pH to 3.0. The resin and the solution were poured into a Sepacol mini column™ (Seikagaku Corporation, Tokyo, Japan), and the column was washed with 5-fold bed volumes of distilled water. The flow-through fraction and the washings were combined and concentrated to dryness by a rotary evaporator. A small amount of distilled water was added to the residue and the solution was lyophilized in a conical tube (Takara, Japan) and applied to the GlycoTag™ for pyridylamination. Excess reagents were removed by extraction twice with 100 μl water-saturated phenol: chloroform (1:1, v/v) followed by extraction with 100 μl chloroform and with 100 μl diethyl-ether.

After suspension of the lyophilized sample in 50 μl of distilled water, the

sample was filtered using 0.2 μm low-binding hydrophilic PTFE membrane Ultrafree^{TM} centrifugal filter (Millipore, Japan) before injection into HPLC columns.

Sugar chain analysis by HPLC

To analyze the expression pattern of both the neutral backbone of the sialylated sugar chains and the unsialylated sugar chains, PA-sugar chains (< 200 pmol) were digested with excess units of neuraminidase in 50 mM acetate buffer solution (pH 5.0) at 37 °C for 18 h (Figure 3). Neutral sugar chains of varying size (in accordance to the number of sugars present on each chain) were separated using an Asahipak NH2P-50 column (4.6×50 mm; Shodex, Tokyo, Japan). Samples were size fractionated from M2 to M11 according to the mannose unit standards M2B, M3, M4B, M5A, M6B, M7A, M8A and M9A (PA-Sugar Chain 057, 016, 058, 017, 018, 052, 019, 020, respectively; Takara, Japan) (Figure 3 and 4). The M10 and M11 elution time was settled as M9 elution time +1.2 and +2.4 min, respectively. Each fraction was subjected to reverse-phase HPLC on a Cosmosil 5C18-P column (4.6×150 mm; Nacalai Tesque, Kyoto, Japan) (Figure 3). Before applying the samples, PA-glucose

oligomer (Takara, Japan), consisting of pyridylaminated isomaltooligosaccharides containing PA-labeled glucose trimer to 22-mer, was injected into the column as external standards of reverse-phase HPLC. The glucose unit (GU) value of each sample peak was calculated by comparing its elution time with those of the two nearest peaks of glucose oligomers. PA-sugar chains were detected by scanning fluorescence detector (FP-2025; Jasco, Japan). Each HPLC step was performed as follows.

Size-fractionation HPLC was performed on an Asahipak NH2P-50 column at a flow rate of 0.6 ml/min at 30℃. Solvent A consisted of 93% acetonitrile, 0.3% acetic acid (pH 7.0), and solvent B consisted of 20% acetonitrile, 0.3% acetic acid (pH 7.0). The column was equilibrated with mixtures of solvents A and B (ratio 97:3). After injecting a sample, proportion of solvent B was increased linearly to 15% in 5 min, to 30% in 25 min, and then 70% in 5 min. PA-sugar chains were detected at an excitation wavelength of 310 nm and emission wavelength of 380 nm (Hase, 1994).

Reverse-phase HPLC was performed on a Cosmosil 5C18-P column at a flow rate of 1.5 ml/min at 30℃. Solvent C consisted of 3.77 mM ammonium acetate buffer (pH 4.0), and solvent D was composed of solvent C containing 0.5% 1-butanol. The

column was equilibrated with a mixture of solvent C and D at a 94:6 ratio. After injecting a sample, proportion of solvent D was increased linearly to 80% in 45 min. PA-sugar chains were detected at an excitation wavelength of 320 nm and emission wavelength of 400 nm.

Quantification of PA-sugar chains

Digital chart recorder, Power Chrom™ (AD Instruments, NSW, Australia) or MacIntegrator™ (Rainin Instruments, MA, USA) system running on Macintosh™ computers (Apple Computer, CA, USA) were used for analysis of area and elution times of each peak. The amount of *N*-linked sugar chains contained in each tissue was quantified by adding the peak areas from all the fractions (M2-M11). The amount of each sugar chain was expressed as the molar percentage of the total *N*-linked sugar chains.

Results

Molecular cloning of glycosidase and glycosyltransferase genes

As a first step to construct the cDNA macroarray, the information of glycosidase and glycosyltransferase genes was obtained from the Genebank. Based on their function, glycosidases and glycosyltransferases are grouped into several families, for example, enzymes that transfer galactose residue to substrate glyco-chains are galactosyltransferases. Molecular cloning of the glycosidase and glycosyltransferase genes enables to further classify them into subfamilies based on their amino acid and nucleic acid sequences. More than 400 glycosyltransferase and glycosidase genes are considered to exist, and among them, more than 130 genes were so far cloned from several species; 127 genes from the mouse, 79 genes from the rat, and 134 genes from the human. Since sequences of some of the mouse genes are not reported, I first tried to obtain mouse homolog for those genes.

Fucosyltransferase: the fucosyltransferase transfers fucose from a donor

GDP-fucose with α1,2-, α1,3- α1,4- or α1,6- linkage (Javaud et al., 2003). While a total of 13 distinct genes have been identified in the human, only ten of them are functional in mice and the mouse homologs for the human FUT 3, 5, and 6 genes were found to be pseudo-genes. Therefore, I cloned the ten functional genes from the mouse cDNA.

Sialyltransferase: the members of this enzyme family transfer sialic acid from a donor CMP-Neuraminic acid to various substrates of glycolipids and glycoproteins with either of α2,3-, α2,6-, or α2,8- linkage (Harduin-Lepers et al., 2001). Twenty genes in this family have been molecularly identified, among which I cloned 19 genes. I could not so far isolate the mouse cDNA for β-galactoside α-2,6-sialyltransferase II, so this gene was not included in the present study.

Galactosyltransferase: the galactosyltransferase enzymes catalyze the transfer of galactose from a donor UDP-galactose to non-reducing residues of glycolipids and glycoproteins with α1,3-, α1,4-, β1,3-, and β1,4-linkage (Amado et al.,

1999). Twenty distinct mammalian genes for the galactosyltransferases (α1,3-GT, α1,4-GT, β1,3-GT I-VIII, β1,4-GT I-VII, glucuronosyltransferase, histo-blood group A transferase and 2 kinds of unclassified β1,3-GT) have been reported in the mouse and human. However, human β1,3-galactosyltransferase VII gene (accession number AF288209) is identical to a DNA sequence reported as β1,3-*N*-acetylglucosaminyltransferase 2 (accession number AF092051). In addition, unclassified human β1,3-galactosyltransferase genes (accession numbers AJ130847 and AJ130848) were identical to genes reported as β1,3-*N*-acetylglucosaminyltransferase 3 and 4, respectively. Therefore, these excessive three genes were removed from a cloning list.

***N*-acetylglucosaminyl (GlcNAc) transferase**: the members of this enzyme family catalyze the transfer of GlcNAc from a donor UDP-GlcNAc to non-reducing terminals of substrates with β1,2-, β1,3-, β1,4-, or β1,6-linkage. To date, more than 26 GlcNAc transferase genes have been reported.

***N*-acetylgalactosaminyl (GalNAc) transferases**: *N*-acetylgalactosaminyltransferases transfer GalNAc from a donor of UDP-GalNAc to various substrates of glycolipids and glycoproteins (Ten et al., 2003). While there are at least 19 distinct mammal GalNAc transferase genes (CSGalNAcT 1, 2, Galgt 1, 2, and GalNAcT 1-14), mouse GalNAcT 8 gene (accession number XM_195594) appears non-functional due to the stop codon in the reading frame. Therefore GalNAcT 8 gene was removed from the cloning list.

Mannosidase: these enzymes catalyze the removal of mannose moieties from glycoproteins (Herscovics, 1999). While 14 different types of mannosidases have been reported in mammals, DNA sequence of Golgi-mannosidases III and ER-mannosidase II have not been reported yet. So these enzymes were removed from the cloning list.

Glucosidase: glucosidases catalyze the removal of glucose residues from glycoproteins and glycolipids (Herscovics, 1999).

I synthesized a pair of primers around the start and stop codons for each gene and performed PCR reactions; DNA fragments were obtained for 85 genes which were reported in the mouse, 3 genes which were cloned from the rat but not from the mouse, and 12 genes whose sequences are only available from the human. Since I could not amplify DNA fragments for 16 genes which are cloned from the human, mouse and rat, I then synthesized another set of degenerative primers for those genes and repeated PCR reactions. As a result, I obtained DNA fragments from total 116 genes, and then subcloned them into a vector plasmid. DNA sequences were examined; the DNA fragments which were cloned based on the mouse sequences were identical to the sequences reported, and the DNA fragments which were cloned based on the rat or human genes showed 80-90% homology to the reported ones. For example, the DNA fragments for β1,4 galactosyltransferase VII gene showed 87.8% homology to the original human gene. I tentatively considered the obtained DNA fragments as homologs to the reported rat or human genes, because the sequences of those fragments showed less homology to any other genes in subfamilies the original gene belongs to. However, it is still possible that the obtained fragments represent a new member of

glycosidase or glycosyltransferase genes. It should also be noted that the isolated DNA fragments cloned based on rat or human sequences may contain some of those original sequences (primers), although those non- mouse sequences were considered to have little effects on results in this study. The cloned genes used in this study are summarized in Table 1. To determine the feasibility of in-house cDNA macroarray system, a set of 116 cDNA clones were spotted onto the nylon membranes using robotic printing, and attempted to identify differentially expressed genes in 12-week postnatal mouse brain compared to age matched kidney and liver, and 12-day fetal brain. Several housekeeping gene, β-actin, GAPDH, ubiquitin B, hypoxanthine phosphoribosyltransferase, myosin 1b, ribosomal protein S29, stroma cell derived factor 4, tyrosine 3-monooxygenase were also printed on the same array to serve as internal controls, and pZErO2 vector and λ DNA as negative control. The example of one such hybridization was shown in Figure 1. The boxed area shows the dilution series of of twelve steps of GAPDH, each corresponding to a 2-fold dilution (Figure 1). The expression level of each genes were determined comparing the intensities of the spots with the expression level of the dilution series (Table 2). cDNA macroarray data

demonstrated that the expression pattern of glycosidases and glycosyltransferases were different among the tissues and during the course of brain development (Figure 1 and Table 2).

Analysis of Tissue Distributions by RT-PCR

To confirm the results of our macroarray, 6 genes were selected and their tissue distributions were analyzed by RT-PCR method (Figure 2). Each of primer pairs and RT-PCR conditions are summarized in Table 3. cDNA macroarray data demonstrated that *N*-acetylglucosaminyltransferase III was expressed in the adult kidney, 12-day embryonic and adult brain. Golgi-mannosidase IB was widely expressed among the all mouse tissues examined. α2,8-sialyltransferase V gene showed adult brain-restricted distribution. β1,3-galactosyltransferase I was expressed at higher levels in the adult liver and brain than in the fetal brain. Fucosyltransferase VIII was expressed at high levels in the 12-day embryonic brain, 12-week postnatal mouse brain, kidney but at low levels in the 12-week postnatal liver. The expression levels of these 6 genes were determined by the RT-PCR method to confirm the differential expression in the mouse tissues, which were consistent with the results

obtained by the macroarray system (Figure 2).

Structural analysis of the major *N*-linked sugar chains expressed in mouse tissues.

In order to know the correlation between the glyco-related gene expression and *N*-glycan expression profiles of each mouse tissue, I analyzed *N*-linked sugar chains by 2 dimensional HPLC following hydrazinolysis and pyridylamination (Fujimoto et al., 1999). Using this established mothod, I determined the content of major *N*-linked sugar chains expressed in the brain from 12-day mouse embryos and in the brain, kidney and liver from 12-week adult mice. More than 40 peaks were fractionated from the PA-labeled sugar chains prepared from each sample by two dimensional HPLC, and each peak was separately collected. The glucose unit (GU) value of each sample peak was calculated by measuring its elution time on reverse-phase HPLC. Each peak collected was re-applied to the second size-fractionation HPLC to fractionate again into several peaks and then to measure precise mannose unit value (MU) of each separated peak. A two-dimensional map of pyridylaminated *N*-linked sugar chains from each mouse tissue sample was thus obtained, which consisted of serial HPLC-separated spots

with two indices; glucose unit (GU) measured by reverse-phase HPLC and mannose unit (MU) measured by size-fractionation HPLC. From these information, I determined the structure of sugar chains by comparing the two-dimensional indicies for each sample with those of standard PA-sugar chains as previously determined (Ikeda, 2003). I could annotate most of the peaks obtained, and this annotation was confirmed by coapplying each peak sample with the standard sugar chains to 2 dimensional HPLC again. The contents of the confirmed *N*-linked sugar chains expressed in the tissues and their structure were summarized in Table 4 and Table 5. During the development of the brain from embryonic day 12 to 12-week adult, content of complex-type sugar chains increased from 18.4% to 23.1% of the total *N*-linked sugar chains, whereas high mannose-type sugar chains decreased their amount from 47.3% to 45.8%. The 12-week adult kidney contained more complex-type sugar chains (25.2%) and less high mannose-type sugar chains (33.2%) than adult liver (16.5% and 52.8%, respectively). Each sugar chain was differentially expressed among the tissues examined. For example, M9 and M8A were highly expressed in the adult liver and 12-day embryonic brain. The amount of M5A was highest in the adults brain. In the kidney, LewisX2-

BA2 and related sugar chains (LewisX-H4 and LewisXa-BA2) were abundantly expressed. A2G2 was highly expressed in the adult liver. Thus, each tissue consistently showed the tissue-specific expression pattern of *N*-linked sugar chain amounts.

Comparison of the expression patterns of *N*-linked sugar chains with the gene expression profiles

Complex type sugar chains containing core fucose structure were present in all tissues, whereas bisecting GlcNAc and LewisX structures were not detected in the adult liver (Table4). Consistently, mRNA of fucosyltransferase VIII (Nishihara et al., 2003) that synthesizes core fucose structures was detectable in all four tissues by cDNA macroarray, which was confirmed by RT-PCR (Figure 2 and Table 4). GnT III (Nishikawa et al., 1992) and fucosyltransferase IX (Uozumi et al., 1996) that catalyze the biosynthesis of bisecting GlcNAc and LewisX structures, respectively, were detected in all tissues except for the adult liver (Table 4). Thus, the results obtained from cDNA macroarray system and *N*-linked sugar chain analysis were very consistent

with each other.

Statistical and comparative analyses of *N*-linked sugar chains and gene expressions

Any tissue from the mouse consists of more than one type of cells, which makes the correlation of the gene expression and *N*-linked sugar chain expression patterns difficult. Therefore, I next analyzed the expression of the glycosidase and glycosyltransferase genes and *N*-glycan in several cell lines. I analyzed 6 cell lines (Neuro2a, NB41A, N1E115, C8D1A, C8D30 and C8S); three are neuroblastoma cells and the others are glioma cells. The results are summarized in Table 6 and 7. Coefficients of the correlation between relative amounts of each *N*-linked sugar chain structure and the relative amounts of each gene mRNA were calculated (Table 8). A cutoff value for the significance was tentatively configurated to 0.8.

Correlations between each *N*-glycan structure

Based on the established *N*-glycan biosynthetic pathways (Figure 5) and the results obtained in our *N*-linked sugar chain analysis that fill the lacking information of

the pathways, I propose the more detailed *N*-glycan biosynthetic pathways (Figure 6). In these pathways, the relative amounts between GM9 and M9 as well as between M9 and M8A showed high correlation coefficients of 0.94 and 0.87, respectively (Table 8). These high correlations are quite reasonable because M9 is considered to be a product of GM9, and M8A a product of M9 in our model of the biosynthesis pathway. In the degradation pathway boxed with a red line in the Figure 6, the relative amounts of M3B, a degradation product of M4, correlated with those of M4 with a coefficient of 0.97, and the relative amounts of M2B, a degradation product of M3B, correlated with those of M3B with a coefficient of 0.98, suggesting that this degradation pathway would be unforked. Besides these results, several pairs of *N*-glycan expression values showed high coefficients more than 0.80. The possible significance will be discussed later.

Correlations between each glyco-gene expression

I found high correlations between some pairs of the relative amounts of glycosyltransferase and glycolipid gene expression examined in the 6 cell lines and the adult liver. For example, the relative expression levels of glucosidase I (Kalz-Fuller et

al., 1995) that catalyze the biosynthesis of G2M9 from G3M9 showed significant correlation with those of glucosidase II (Grinna et al., 1980) that synthesizes M9 from G2M9 with a coefficient of 0.82 (Figure 6 and Table 8), although they are distinct in their structures and show little homology to each other. The relative amounts of GnT I (Kumar et al., 1990) that adds GlcNAc to M5A to yield H5 highly correlated with those of GnT II (D'Agostaro et al., 1995) that also adds GlcNAc to A1(3)G0 to produce A2G0 with a coefficient of 0.87 (Figure 6 and Table 8). However, the relative expression levels of mannosidase II (Moremen et al., 1991) that catalyzes a biosynthesis step between the GnT I and GnT II reactions showed no correlation with GnT I nor GnT II (Figure 6 and Table 8).

Correlations between *N*-glycan and glyco-relate gene expression

The relative amounts of Gal-H5 *N*-glycan structure and mannosidase II gene expression demonstrated a significant inverted correlation (Table 8). This would be explained by a competition mechanism between mannosidase II that utilizes H5 as a substrate to produce A1(3)G0 structure and β1,4-galactosyltransferase that also utilizes

H5 as a substrate to synthesize Gal-H5 structure (Figure 6).

Discussion

Development of the cDNA macroarray system

DNA array technology allows simultaneous measurement of the expression levels of many genes (Duggan et al., 1999). This provides both static information about expression of each gene, and dynamic information on how their individual levels of expression relate to one another within the array. However, for the purposes of the present study, commercially available microarrays presented major drawbacks as regarding the number of genes spotted onto the slide glass and the detection sensitivity. Especially the latter would limit the usefulness of the array technology, because the expression of glycosyltransferase and glycosidase genes were generally low. For example, I tried a DNA chip provided by TaKaRa IntelliGene to find that only 8 glycosyltransferase genes on the chip showed detectable differences in their expression among four different tissues (data not shown).

In this work, I have developed a cDNA macroarray system capable of evaluating the expression of many glycosidase and glycosyltransferase genes

simultaneously with high sensitivity. I utilized radioactive labeling coupled with a phosphor-imager detection system, instead of the fluorescence-based labeling used in the microarray system. The very good signal/noise ratios of the individual spots obtained by the hybridization procedures with highly stringent conditions and visualized by the phosphor-imager that itself enhances the detection sensitivity up to 100 times more than a conventional film technology, demonstrated that the macroarray was suitable for simultaneous glyco-gene expression analyses (Figure 1). At the same time, in the hand-made macroarray system, I could spot as many as 116 glycosyltransferase and glycosidase genes, which encompass most of the genes associated in the biosynthesis and degradation of *N*-linked glycochains. By comparing the expression levels of glyco-genes to that of one of the housekeeping genes, GAPDH gene, whose expression levels are relatively stable in all tissues used in this study, I succeeded in normalizing the gene expression values of each array and semi-quantifying amounts of mRNA for each gene spotted onto the membranes. I applied this technology to analyze the glyco-gene expression profiles in various types of tissues and cell lines.

Application of the cDNA macroarray system

The method was successfully applied to examine the gene expression levels related to the *N*-linked sugar chain biosynthesis in the mouse tissues and cell lines. While previous studies usually analyzed only one or two glyco-genes in relation to amounts of their substrates and products of *N*-glycan, I simultaneously examined the levels of the 116 glyco-genes and determined most of the *N*-glycan structures, which could provide quite new insights to the regulatory mechanisms of *N*-linked sugar chains. Some of the examples are described below.

Expression of glycosidase genes are under a shared regulatory system

The relative mRNA amounts of glucosidase I and II, which shares similar enzymatic activities but show no homology in their amino acid sequences, showed a high correlation (coefficient of 0.82). In addition, the amounts of glucosidase I and II mRNA showed high correlation with those of ER-mannosidase mRNA (coefficients of 0.84 and 0.74, respectively) as well as Golgi-mannosidase IB mRNA (coefficients of 0.89 and 0.92, respectively), but showed less correlation with GnT II mRNA level

(coefficients of 0.50 and 0.69, respectively). These observations suggest that the expression of the genes which reside in the endoplasmic reticulum or *cis*-Golgi apparatus and catalyze early *N*-glycan biosynthesis, are under shared regulatory mechanisms. Comparison of the promoter regions of those genes may reveal the presence of similar promoter elements or structures. The inverse correlations found between the relative amounts of glucosidase II mRNA levels and M9A glyco-chain (coefficient of -0.81) appear at odd when considering that GM9 and M9A are catalytic products of glucosidase I and II, respectively. However, since the expression of glucosidase I and II and ER-mannosidase were under the coordinated regulation, these three enzymes may be considered as an integrated machinery to produce *N*-glycans within the *cis*-Golgi body (M7A and B and M6B). Indeed, the relative total amounts of M7A and B and M6B well correlated with the relative expression levels of glucosidase I and ER-mannosidase (coefficients of 0.65 and 0.87, respectively). Alternatively, the inverse correlation between glucosidase II mRNA levels and M9 amounts might be interpreted as a result of feedback regulatory mechanisms (see below).

Implication of the inverse correlation between glucosidase II and M9 structure

The biosynthesis and maturation of *N*-glycans occurs within the membranes of the endoplasmic reticulum (ER) and the Golgi complex. G3M9 structure is initially transferred to form an amide linkage to Asn side chains of newly synthesized polypeptides as they are co-translationally translocated through the ER membrane. Irrespective of protein conformation, the glucose residues of the glycan are removed by glucosidase I, and then by glucosidase II (Grinna et al., 1980, Pelletier et al., 2000). Membrane-bound calnexin and its lumenal homolog calreticulin (lectin-like molecular chaperones (Schrag et al., 2003)) interact specifically with glycoproteins bearing the glycan processing intermediate GM9 (Zapun et al., 1997). Dissociation of the glycoprotein from calnexin permits the cleavage of the remaining glucose residues by glucosidase II, yielding M9. If glycoproteins are adequately folded to take an appropriate tertiary structures, they are exported from the ER by vesicular transport. In contrast, if glycoproteins are aberrantly folded, it is recognized by UDP- glucose glycoprotein glucosyltransferase (UGGT), which catalyzes the transfer of a glucose

moiety from UDP-glucose to specific mannose residues. Re-synthesis of the GM9 allows aberrantly folded glycoproteins to re-associate with calnexin (Pelletier et al., 2000; Sousa et al., 1992).

Within this biosynthetic pathway, the inverse correlation between glucosidase II mRNA levels and M9 amounts (correlation coefficient of -0.81) seems interesting. Since the quality control of the glycoprotein is performed at the M9-bearing stage reaction from GM9 to M9, M9 to GM9 that UGGT catalyzes are very important for the quality contorol of the glycoproteins, increase of M9 to an excess amount may not be preferable for strict quality control. Thus, the transcription of glucosidase II gene is needed in M9-bearing glycoproteins through unknown feedback mechanisms by M9.

_N_-glycan expression patterns are distinct between tissue and cell lines

Since the brain consists of neurons, astrocytes, oligodendrocytes, and other minor population of cells, amounts of *N*-liked sugar chains would be sum of the glyco-chains expressed on each cell type, which makes it difficult to analyze regulatory

mechanisms underlying biosynthesis of *N*-liked sugar chains. Therefore, we next examined *N*-liked sugar chain amounts and glyco-gene expression profiles of neuronal and astrocytic cell lines, expecting that these cells might reflect the *N*-liked sugar chain and glyco-gene patterns of the brain. However, the cell lines, three neuroblastoma and three astrocytoma cell lines, showed totally different *N*-liked sugar chain patterns from the brain; neither of the cells expressed LewisX, bisecting GlcNAc, or core fucose structures, which are relatively rich in the brain. Instead, these cell lines expressed A2, A3 and A4 types of *N*-glycan in large amounts. These types of sugar chains were often observed rich in tumor cells (unpublished data). It was reported that A3 and A4 types of *N*-linked sugar chains and the expression levels of GnT4 and GnT5 genes that synthesize A3 and A4, respectively, were increased in parallel in cancer cells (Yamashita et al., 1985; Pierce et al., 1997). Similarly, M2B and M3B, which were abundantly expressed in the astrocytoma cell lines were barely detected in the brain. The differences of the *N*-liked sugar chain profiles between the brain and the cell lines could be explained by at least three possibilities. The distinct patterns of *N*-glycan in the cell lines from that in the brain may reflect tumorous characteristics of the cells,

may result from the lack of 3D structures, or may be due to the lack of interaction between neurons and glia. Alternatively, the neuroblastoma and astrocytoma cells may be too immature to express brain-specific *N*-glycan patterns. Indeed, Osanai et al. revealed that the LewisX-bearing glycolipds were increased in amount during the course of neuronal differentiation of P19 embryonic carcinoma cells induced by retinoic acid (Osanai et al., 2001).

Significant role of mannosidase II in the biosynthesis of complex and hybrid type *N*-glycans

Mannosidase II catalyzes the production of A1(3)G0 from H5, a key intermediate product of both complex and hybrid type *N*-glycans. It would be supposed that the more mannosidase II gene is expressed, the more complex type *N*-glycans produced, and in contrast, the less hybrid type *N*-glycans yielded. Indeed, the mannosidase II expression levels and hybrid type *N*-glycan (Gal-H5) amounts showed inverse correlation (coefficient of –0.84). Terminal sugar moieties are supposed to play significant roles in the cell-to-cell interactions. Because complex and hybrid type

N-glycans differ in the numbers of branches, hense the terminal moieties. For example, one of complex *N*-glycans A4G4 contains 4 terminal structures of Gal-GlcNAc, whereas hybrid type Gal-H5 possesses only one. These differences may result in different cell behavior to interact with other cells. It would be intriguing to investigate behavior of cells, in which mannosidase II is differently expressed.

Chain reactions of glycosyltransferases

Although highly branched complex type *N*-glycans, A4G4 and A4G4F, were observed in several cell lines, their intermediate products, A3G0 and A4G0, were not detected in the same cell lines. Galactosyltransferases that catalyze an addition of galactose to terminal GlcNAc residues could be expressed in excess amounts or their reaction velocities could be very rapid. Alternatively, GnTs that synthesize A3G0(F), and then A4G0(F) might exist in couple with the galactosyltransferases. In this case, the enzymes that catalyze a series of *N*-glycan biosynthesis may be located in a small compartment or form the complex machinery.

Conclusion

In this study, I utilized the cDNA macroarray system and 2 dimensional HPLC analysis of *N*-linked sugar chains to examine normal mouse tissue and cell lines. If these systems are applied to pathological specimen (cancerous tissues for example), aberrant patterns of gene and *N*-glycan expression profiles may be obtained, which might clarify the pathogenesis of the cancer and mechanisms of its metastasis. My study will open a new research field in glycobiology.

Acknowledgements

I wish to express my gratitude to many people in completing my thesis and research during these three years.

Prof. K. Ikenaka, my supervisor and head of Laboratory of National Institute of Physiological Sciences, Okazaki National Research Institutes. I would like to thank him specially for introducing me such an exciting theme as glycobiology and for his valuable guidance throughout this study.

Dr. Seiji Hitoshi and Dr. I. Fujimoto. I would like to thank them for reading the draft and making a number of helpful suggestions.

Prof. S. Hase and Dr. S. Nakakita, Department of Chemistry, Graduate School of Science, Osaka University. I wish to thank them for various help and valuable advices.

Prof. N. Ueno and Dr. A. Kitayama, Division of morphogenesis, National Institute for Basic Biology. I would like to thank them for allowing me to use the cDNA macroarray spotting machine and their instruction over cDNA macroarray analysis.

I thank my colleagues for useful discussions, especially Dr. T. Ikeda, Mr. K Tanabe Dr. A. Deguchi, Mr. K. Sakuma and Mr. G. Yamada.

Finally, I thank Ms. I. Ito for her technical assistance on HPLC analysis.

References

Albach C, Klein RA, Schmitz B. (2001) Do rodent and human brains have different *N*-glycosylation patterns. *Biol. Chem.,* **382**, 187-194.

Allendoerfer KL, Durairaj A, Matthews GA, Patterson PH. (1999) Morphological domains of Lewis-X/FORSE-1 immunolabeling in the embryonic neural tube are due to developmental regulation of cell surface carbohydrate expression. *Dev. Biol.,* **211**, 208–219.

Amado M, Almeida R, Schwientek T, Clausen H. (1999) Identification and characterization of large galactosyltransferase gene families: galactosyltransferases for all functions. *Biochimica et Biophysica Acta.,* **1473**, 35-53.

Chen YJ, Wing DR, Guile GR, Dwek RA, Harvey DJ, Zamze S. (1998) Neutral *N*-glycans in adult rat brain tissue: Complete characterisation reveals fucosylated hybrid

and complex structures. *Eur. J. Biochem.,* **251**, 691-703.

D'Agostaro GA, Zingoni A, Moritz RL, Simpson RJ, Schachter H, Bendiak B. (1995) Molecular Cloning and Expression of cDNA Encoding the Rat UDP-*N*-Acetylglucosamine: α-6- D-Mannoside -1,2-*N*-Acetylglucosaminyltransferase II. *J. Cell Biol*., **270**, 15211-15221.

Duggan DJ, Bittner M, Chen Y, Meltzer P, Trent JM. (1999) Expression profiling using DNA microarrays. *Nat. Genet.,* **21 (Suppl 1)**, 10-14.

Fujimoto I, Menon KK, Otake Y, Tanaka F, Wada H, Takahashi H, Tsuji S, Natsuka S, Nakakita S, Hase S, Ikenaka K. (1999) Systematic analysis of *N*-linked sugar chains from whole tissue employing partial automation. *Anal. Biochem.,* **267**, 336-343.

Geetha-Habib M, Noiva R, Kaplan HA, Lennarz WJ. (1988) Glycosylation site binding protein, a component of oligosaccharyl transferase, is highly similar to three other 57 kd

luminal proteins of the ER. *Cell,* **54,** 1053–1060.

Grinna LS, Robbins PW. (1980) Substrate specificities of rat liver microsomal glucosidases which process glycoproteins. *J. Biol. Chem.,* **255**, 2255-2258.

Harduin-Lepers A, Vallejo-Ruiz V, Krzewinski-Recchi MA, Samyn-Petit B, Julien S, Delannoy P. (2001) The human sialyltransferase family. *Biochimie.,* **83**, 727-737.

Hase S, Ikenaka T, Matsushima Y. (1981) A high sensitive method for analysis of sugar moieties of glycoproteins by fluorescence labeling. *J. Biochem.,* **90**, 407-414.

Hase S, Natsuka S, Oku H, Ikenaka T. (1987) Identification method for twelve oligomannose-type sugar chains thought to be processing intermediates of glycoproteins. *Anal. Biochem.,* **167**, 321-326.

Hase S, Ikenaka K, Mikoshiba K, Ikenaka T. (1988) Analysis of tissue glycoprotein

sugar chains by two-dimensional high-performance liquid chromatographic mapping. *J. Chromatogr.,* **434**, 51-60.

Helenius A, Aebi M. (2001) Intracellular functions of *N*-linked glycans. *Science*, **291**, 2364-2369.

Herscovics A. (1999) Importance of glycosidases in mammalian glycoprotein biosynthesis. *Biochimica et Biophysica Acta.,* **1473**, 96-107.

Ikeda T. (2003) Characterization of majour *N*-linked sugar chain structures expressedin mouse cerebral cortex duringdevelopment. Thesis for doctoral degree.

Javaud C, Dupuy F, Maftah A, Julien R, Petit JM. (2003) The Fucosyltransferase Gene Family: An Amazing Summary of the Underlying Mechanisms of Gene Evolution. *Genetica*., **118**, 157-170.

Jenkins N, Parekh RB, James DC. (1996) Getting the glycosylation right: implications for the biotechnology industry. *Nat. Biotechnol.,* **14,** 975–981.

Kalz-Fuller B, Bieberich E, Bause E. (1995) Cloning and expression of glucosidase I from human hippocampus. *Eur J Biochem.,* **231**, 344-351.

Kornfeld R, Kornfeld S. (1985) Assembly of Asparagine-Linked Oligosaccharides. *Annu. Rev. Biochem.,* **54,** 631–664.

Kumar R, Yang J, Larsen RD, Stanley P. (1990) Cloning and expression of *N*-acetylglucosaminyltransferase I, the medial Golgi transferase that initiates complex *N*-linked carbohydrate formation. *Proc Natl Acad Sci U S A.,* **87**, 9948-9952.

Liu Y, Choudhury P, Cabral CM, Sifers RN. (1999) Oligosaccharide modification in the early secretory pathway directs the selection of a misfolded glycoprotein for degradation by the proteasome. *J. Biol. Chem.,* **274**, 5861-5867.

Moremen KW, Robbins PW. (1991) Isolation, Characterization, and Expression of cDNAs Encoding Murine α-Mannosidase II, a Golgi Enzyme That Controls Conversion of High Mannose to Complex *N*-Glycans. *J. Cell Biol*., **115**, 1521-1534.

Nishihara S, Iwasaki H, Nakajima K, Togayachi A, Ikehara Y, Kudo T, Kushi Y, Furuya A, Shitara K, Narimatsu H. (2003) α1,3-Fucosyltransferase IX (Fut9) determines Lewis X expression in brain. *Glycobiology*, **13**, 445-455.

Nishikawa A, Ihara Y, Hatakeyama M, Kangawa K, Taniguchi N. (1992) Purification, cDNA Cloning, and Expression of UDP-*N*-acetylglucosamine: β-D-mannoside β-1,4N-Acetylglucosaminyltransferase III from Rat Kidney. *J. Biol. Chem.,* **261**, 18199-18204.

Orlean P. (1992) Enzymes that recognize dolichols participate in three glycosylation pathways and are required for protein secretion. *Biochem.Cell Biol.,* **70,** 438–447.

Osanai T, Chai W, Tajima Y, Shimoda Y, Sanai Y, Yuen CT. (2001) The LewisX bearing glycolipds were increased in amounts during the course of neural differentiation of P19 EC cells induced by retinoic acid. *FEBS letters,* **488**, 23-28.

Otake Y, Fujimoto I, Tanaka F, Nakagawa T, Ikeda T, Menon KK, Hase S, Wada H, Ikenaka K. (2001) Isolation and characterization of an *N*-linked sugar oligosaccharide that is significantly increased in sera from patients with non-small cell lung cancer. *J. Biochem.,* **129**, 537-542.

Pelletier MF, Bergeron JJ, M. & Thomas DY. (2000) Molecular chaperone systems in the endoplasmic reticulum. *In Molecular Chaperones in the Cell*. 180-200.

Pelletier MF, Marcil A, Sevigny G, Jakob CA, Tessier DC, Chevet E, Menard R, Bergeron JJ, Thomas DY. (2000) The heterodimeric structure of glucosidase II is required for its activity, solubility and localization *in vivo*. *Glycobiology,* **10**, 815-827.

Pierce M, Buckhaults P, Chen L, Fregien N. (1997) Regulation of *N*-acetylglucosaminyltransferase V and Asn-linked oligosaccharide β(1,6) branching by a growth factor signaling pathway and effects on cell adhesion and metastatic potential. *Glycoconj J.,* **14**, 623-630.

Ronn LC, Berezin V, Bock E. (2000) The neural cell adhesion molecule in synaptic plasticity and ageing. *Int. J. Dev. Neurosci.,* **18**, 193–199.

Schrag JD, Procopio DO, Cygler M, Thomas DY, Bergeron JJ. (2003) Lectin control of protein folding and sorting in the secretory pathway. *Trends Biochem. Sci.,* **28**, 49-57.

Sousa MC, Ferrero-Garcia MA, Parodi AJ. (1992) Recognition of the oligosaccharide and protein moieties of glycoproteins by the UDP-Glc: glycoprotein glucosyltransferase. *Biochemistry,* **31**, 97-105.

Spiro MJ, Spiro RG. (1991) Potential Regulation of *N*-Glycosylation Precursor through

Oligosaccharide-Lipid Hydrolase Action and Glucosyltransferase-Glucosidase Shuttle. *J. Biol. Chem.,* **266**, 5311–5317.

Ten Hagen KG, Fritz TA, Tabak LA. (2003) All in the family: the UDP-GalNAc: polypeptide *N*-acetylgalactosaminyltransferases. *Glycobiology,* **13**, 1R-16R.

Uozumi N, Yanagidani S, Miyoshi E, Ihara Y, Sakuma T, Gao CX, Teshima T, Fujii S, Shiba T, Taniguchi N. (1996) Purification and cDNA Cloning of Porcine Brain GDP-L-Fuc: *N*-Acetyl-β-D-Glucosaminide α1,6Fucosyltransferase. *J. Biol. Chem.,* **271**, 27810-27817.

Yamashita K, Tachibana Y, Ohkura T, Kobata A. (1985) Enzymatic basis for the structural changes of asparagine-linked sugar chains of membrane glycoproteins of baby hamster kidney cells induced by polyoma transformation. *J. Biol. Chem.,* **260**, 3963-3969.

Zamze S, Harvey DJ, Chen YJ, Guile GR, Dwek RA, Wing DR. (1998) Sialylated *N*-glycans in adult rat brain tissue: a widespread distribution of disialylated antennae in complex and hybrid structures. *Eur. J. Biochem.,* **258**, 243-270.

Zapun A, Petrescu SM, Rudd PM, Dwek RA, Thomas DY, Bergeron JJ. (1997) Conformation-independent binding of monoglucosylated ribonuclease B to calnexin. *Cell,* **88**, 29-38.

Figure 1. Representative results of the cDNA macroarray.

Each membrane contains quadicated spots for 116 genes genes of cDNA fragments, which were implicated in the biosynthesis of sugar chains. mRNA from four mouse tissue samples, 12-day embryonic brain, 12-week postnatal brain, kidney and liver were prepared and then used to synthesize cDNA probes labeled with ^{32}P-dCTP. Each probe was hybridized to a cDNA expression macroarray, and images were obtained by exposing the arrays to an imaging plate. For the semi-quantitative analysis, the same arrays were exposed to the imaging plates to measure the radioactivity with a BAS 1800II imaging analyzer. The spots surrounding the filter (the boxed area with a green line) are diluted GAPDH for identification of the gene position. The boxed area with a red line show the glyco-related gene spotted area. The boxed area with a black line shows the dilution series of GAPDH consisting of ten steps, each corresponding to a 2-fold dilution. (a) embryonic 12 day brain (b) postnatal 12 week brain (c) kidney (d) Liver

Figure 2. Expression profiles of 6 selected genes.

Gene expressions were analyzed by RT-PCR using mRNAs from 4 mouse tissues (brain from 12-day embryo, and brain, liver kidney from 12-week adult mice) Each primers set and PCR condition were summarized in Table 3. cDNA macroarray data demonstrated that *N*-acetylglucosaminyltransferase III was expressed in the adult kidney, 12-day embryonic and adult brain. Golgi-mannosidase IB was widely expressed among the all mouse tissues examined. α2,8-sialyltransferase V gene showed adult brain-restricted distribution. β1,3-galactosyltransferase I was expressed at higher levels in the adult liver and brain than in the fetal brain. Fucosyltransferase VIII was expressed at high levels in the 12-day embryonic brain, 12-week postnatal mouse brain, kidney but at low levels in the 12-week postnatal liver. The expression levels of these 6 genes were determined by the RT-PCR method to confirm the differential expression in the mouse tissues, which were consistent with the results obtained by the macroarray system (Figure 2).

Figure 3. Outline of the general strategy employed in this study.

Tissues and cell line samples were homogenized with nine-fold volume of acetone, and

the precipitates were lyophilized. Samples were hydrazinolized to release sugar chains and then *N*-acetylated. These steps were performed manually. The amount of samples for hydrazinolysis was 2 mg. After lyophilization, sugar chains were converted to pyridylamino (PA) derivatives by the automated GlycoTag^{TM}. Excess reagents were removed by phenol:chloroform (1:1) extraction. The sugar chain backbone of the PA-sugar chains containing sialylated and neutral components was totally detected by two-dimensional HPLC (size-fractionation HPLC and reverse-phase HPLC) after neuraminidase digestion.

Figure 4. Two-dimensional HPLC analysis of PA-sugar chains.

PA-sugar chains were detected by the fluorescence detector at femtomole levels, and excellent separation was achieved by a combination of size-fractionation HPLC and reverse-phase HPLC. Sugar chain backbones of neuraminidase-treated PA-sugar chains were analyzed by two-dimensional HPLC composed of size-fractionation HPLC and reverse-phase HPLC. Any impurities of non-sugar nature, if present in these fractions, were removed along with the flow thorough. Size fractionation was

performed by collecting nine samples at the elution time of the mannose unit standards M2B, M3B, M4B, M5A, M6B, M7A, M8A and M9A (see Table 5). The M10 and M11 were sequentially fractionated during 1.2 min from M9 fraction end time. These individual fractions were further characterized by a Cosmosil 5C18-P reverse-phase HPLC column. The PA-sugar chains were detected at an excitation wavelength of 320 nm and an emission wavelength of 400 nm. Essentially all of the *N*-linked sugar chains elute after 10 min, while O-linked sugar chains are partially recovered using our procedures and elute earlier together with impurities.

Figure 5. The major biosynthetic pathways of *N*-linked sugar chains in mammalian cells.

The enzymes are indicated in the digit; ①Glucosidase I ②Glucosidase II ③ER-Mannosidase I ④ER-Mannosidase II ⑤Endo-Mannosidase ⑥Golgi-Mannosidase IA ⑦Golgi-Mannosidase IB ⑧Golgi-Mannosidase IC ⑨GnT I ⑩Mannosidase II ⑪GnT II ⑫Fuc-T VIII ⑬β1,4GTs ⑭GnT 4A, 4B, 4H ⑮GnT V ⑯ β1,3GTs

Figure 6. The biosynthetic pathways of *N*-linked sugar chains in cell lines

The enzymes are indicated in the digit; ①Glucosidase II ②ER-Mannosidase I ③ Golgi-Mannosidase IB ④GnT I ⑤Mannosidase II ⑥GnT II ⑦FuT VIII ⑧β1,4Gal Ts ⑨GnT 4A, 4B ⑩GnT V ⑪β1,3GTs

Table1.The list of genes used in this study

The glycosidases and glycosyltransferases are grouped mainly into 7 families.

Table2.The result of gene expression analysis

The mRNA levels of glycosidases and glycosyltransferases were analyzed in four mouse tissue samples, 12-day fetal brain, 12-week postnatal brain, kidney and liver. The mRNA level of each gene was determined by comparing their intensities with those of the dilution series of GAPDH.

Table3. Primer Pairs and PCR Conditions

GnTIII, N-acetylglucosaminyltransferase III; 2,8-ST V, 2,8-sialyltransferase V; ManIB, Golgi-mannosidase IB; b1,3GT I, b1,3-galactosyltransferase 1; Fuc-T VIII, fucosyltransferase VIII; Fuc-T IX, fucosyltransferase IX; GAPDH, glyceraldehyde-3-phosphate dehydrogenase. Note. Template cDNAs for RT-PCR were synthesized from

200ng of poly(A)+ RNAs using 200 U Superscipt II reverse and random(N6) primers. PCRs were carried out using 0.25U Taq DNApolymerase, 200 μM dNTP, 2 μM each primer sets, and the template cDNAs. PCR conditions were as follows; after incubation for 5 min at 96 ˚C, 25-35 cycles of denaturing at 96 ˚C for 45 s, annealing at 60 ˚C for 45 s, extention at 72 ˚C for 90s, and then final extention at 72 ˚C for 7min.

Table4.Structures of desialylated *N*-glycan derived from several tissues

Major *N*-linked sugar chains expressed in mouse tissue. The nomenclature of the sugar chains is shown in “Abbreviations” and Table 5. The values shown are the relative abundances (RA) against total *N*-linked sugar chains from M2 to M11 fraction.

Table5.Structures and abbreviations of PA-sugar chains.

Table6. Structures of desialylated *N*-linked sugar chains derived from cell lines and adult liver.

N-linked sugar chains expressed in 6 cell lines and adult liver. The nomenclature of

the sugar chains is shown in “Abbreviations” and Table 5. The values shown are the relative abundances (RA) against total *N*-linked sugar chains from M2 to M11 fraction.

Table7. The gene expression analysis of 6 cell lines and adult liver.

The gene expressions of glyco-related gene were analyzed in six mouse cell lines(Neuro2a, NB41A, N1E115, C8D1A, C8D30, C8S) and adult liver.

Table8 :The correlation between *N*-linked sugar chins and gene expression.

Correlation coefficient between relative amount of each N-glycan and the relative amounts of each glyco-related gene mRNA was calculated. A cutoff value for the significance was tentatively configulated to 0.8

Figure 1

(a)

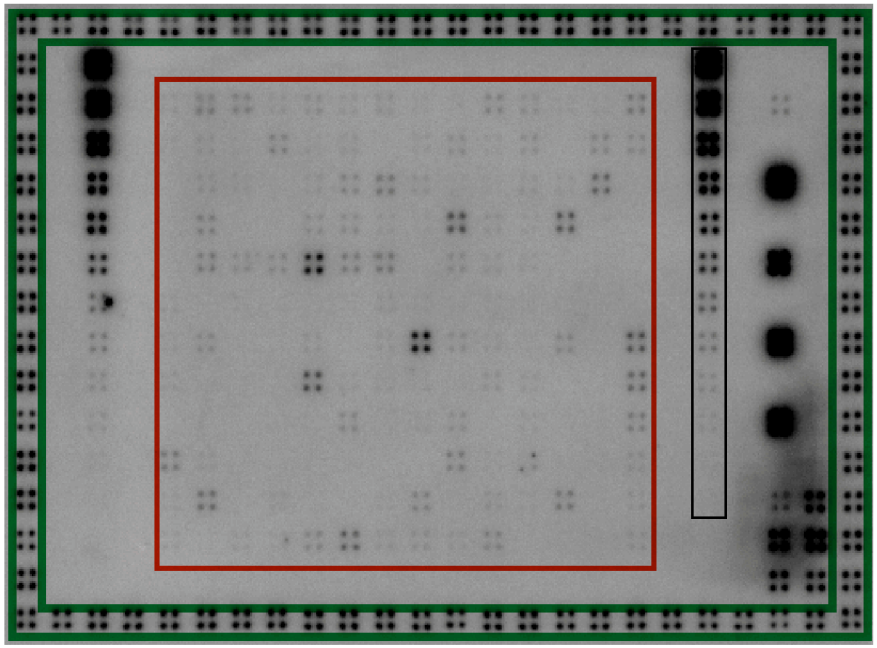

(b)

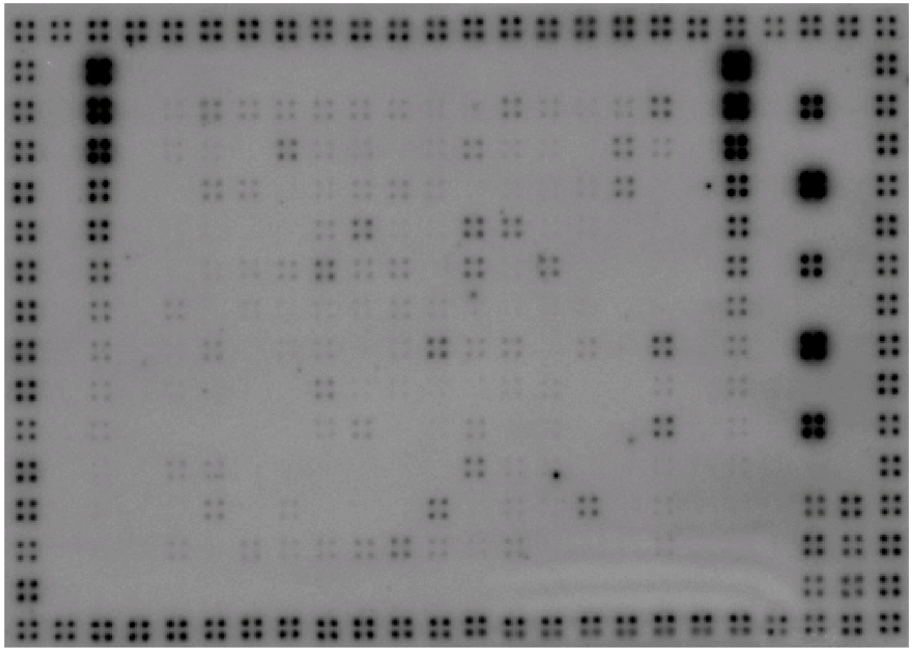

(c)

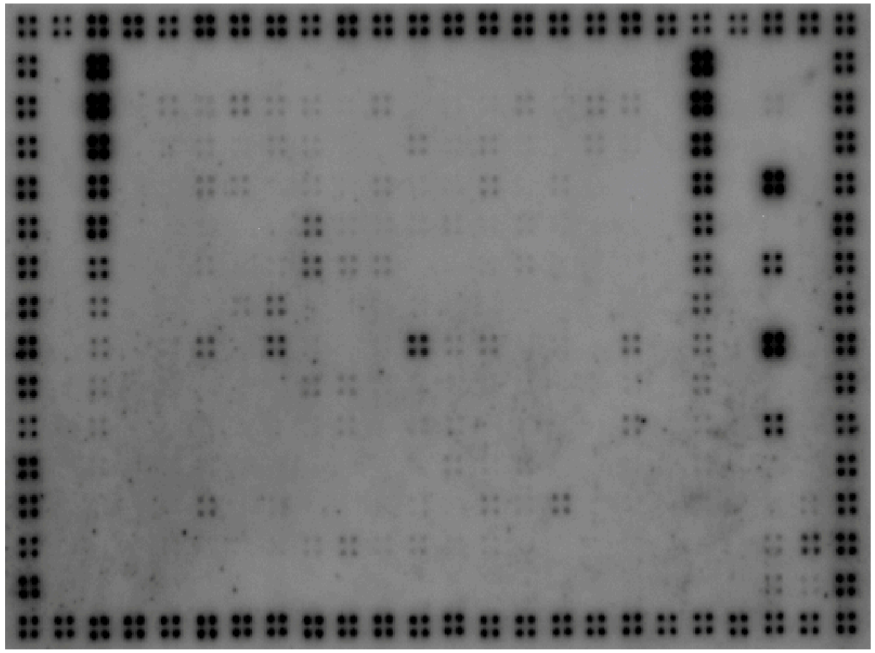

(d)

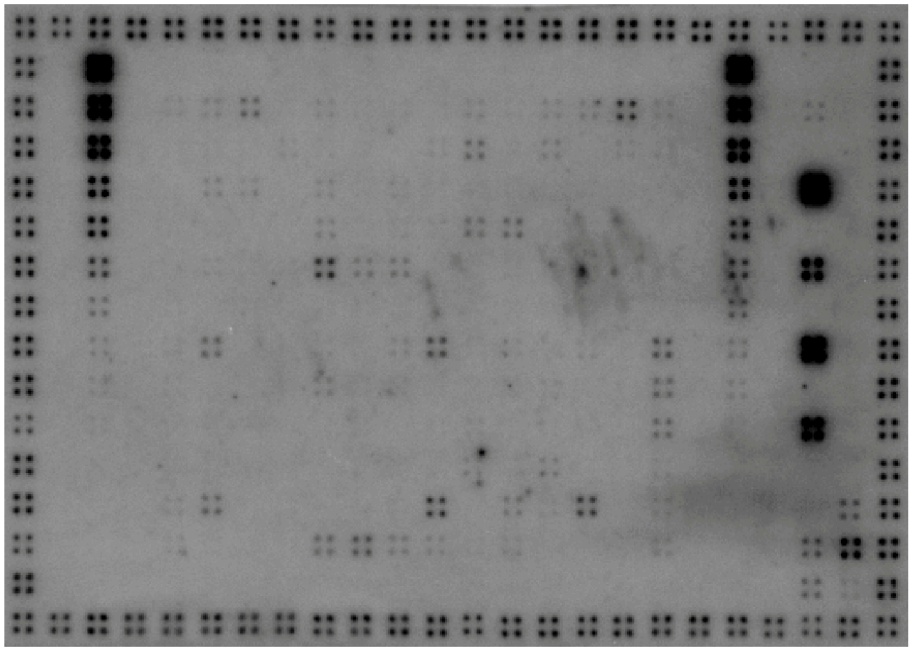

Figure 2

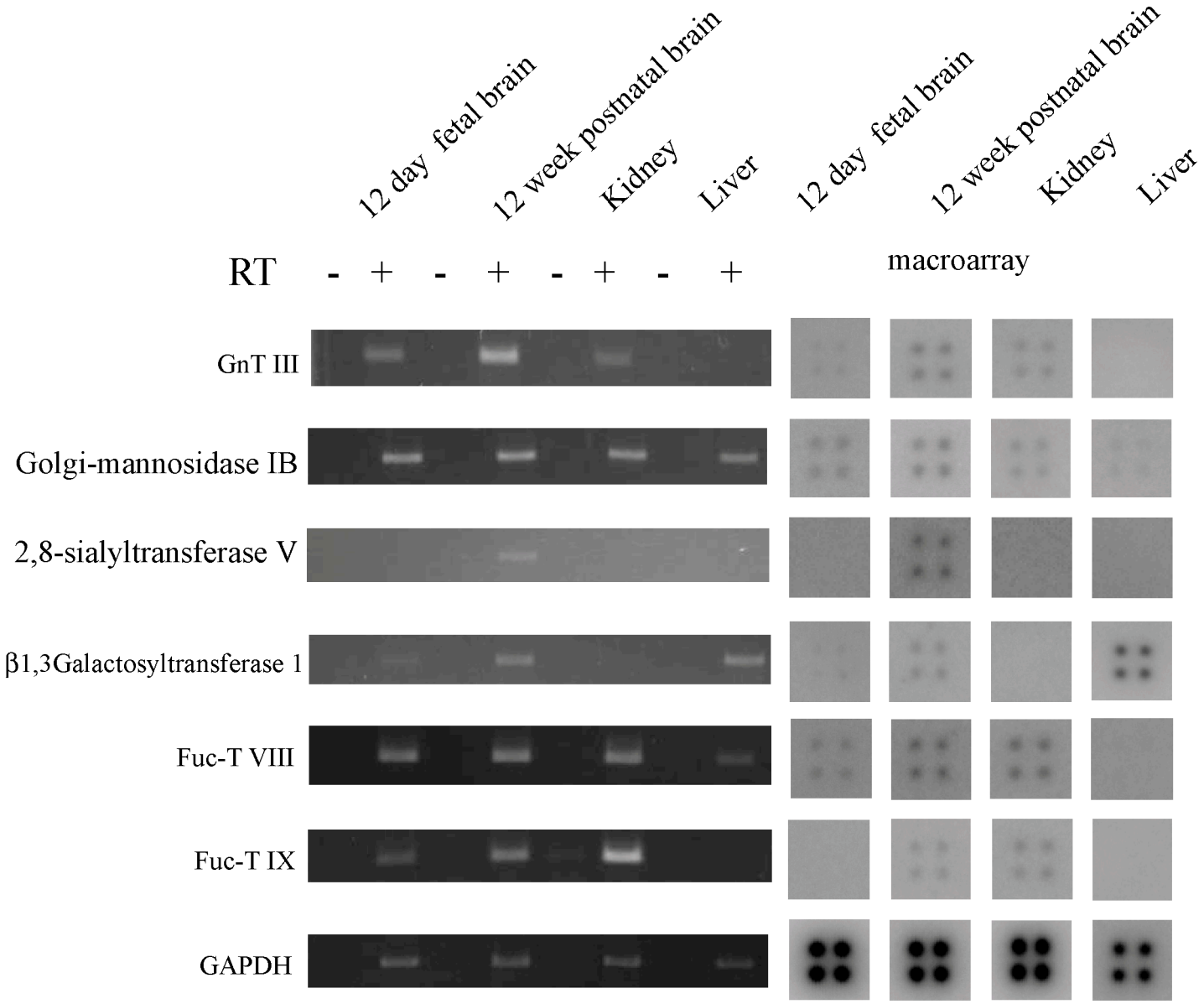
12 day fetal brain
12 week postnatal brain
Kidney
Liver
12 day fetal brain
12 week postnatal brain
Kidney
Liver
RT - + - + - + - +
macroarray
GnT III
Golgi-mannosidase IB
2,8-sialyltransferase V
β1,3Galactosyltransferase 1
Fuc-T VIII
Fuc-T IX
GAPDH

Figure 3

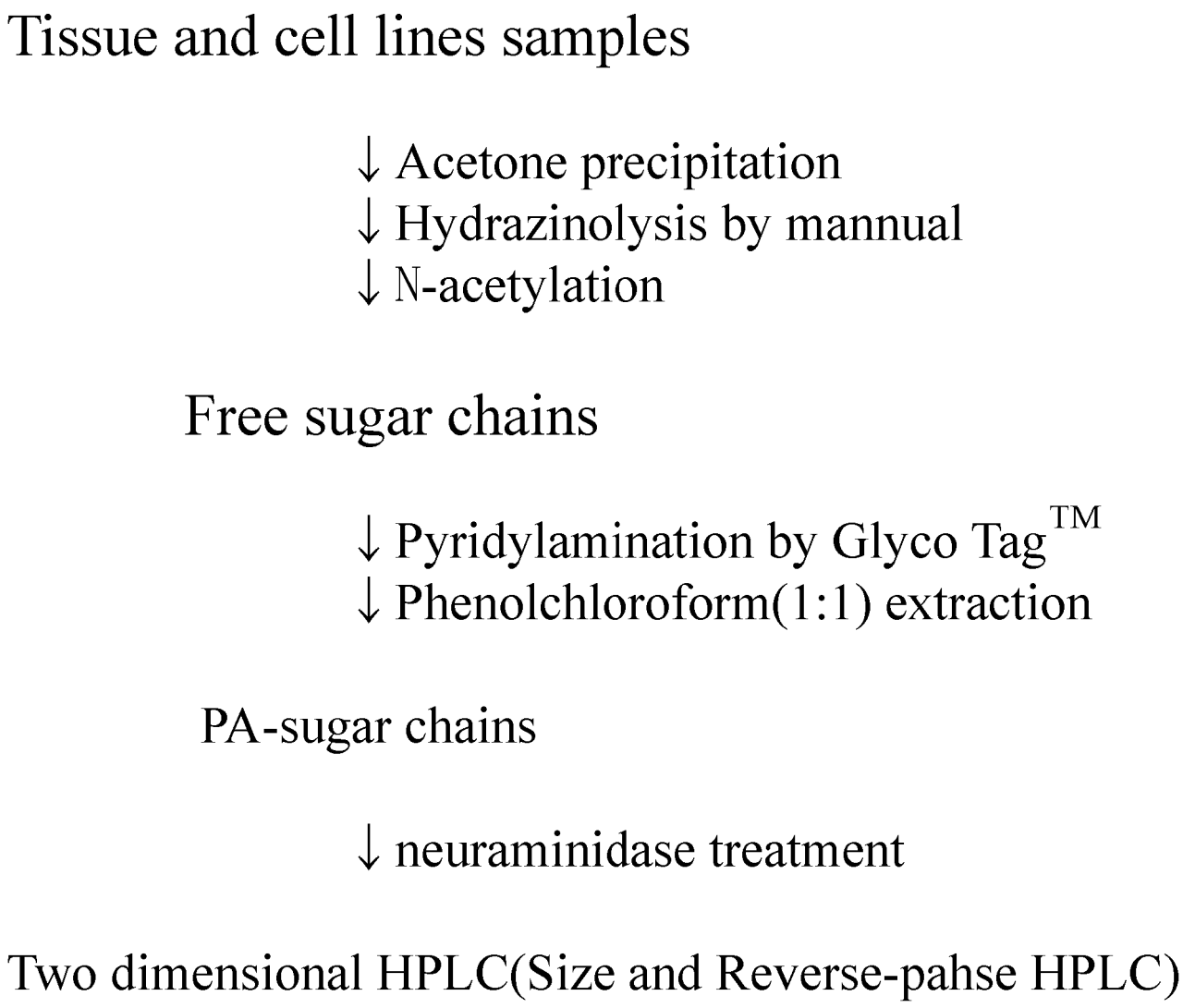
Tissue and cell lines samples
↓ Acetone precipitation
↓ Hydrazinolysis by mannual
↓ N-acetylation
Free sugar chains
↓ Pyridylamination by Glyco Tag™
↓ Phenolchloroform(1:1) extraction
PA-sugar chains
↓ neuraminidase treatment
Two dimensional HPLC(Size and Reverse-pahse HPLC)

Figure 4

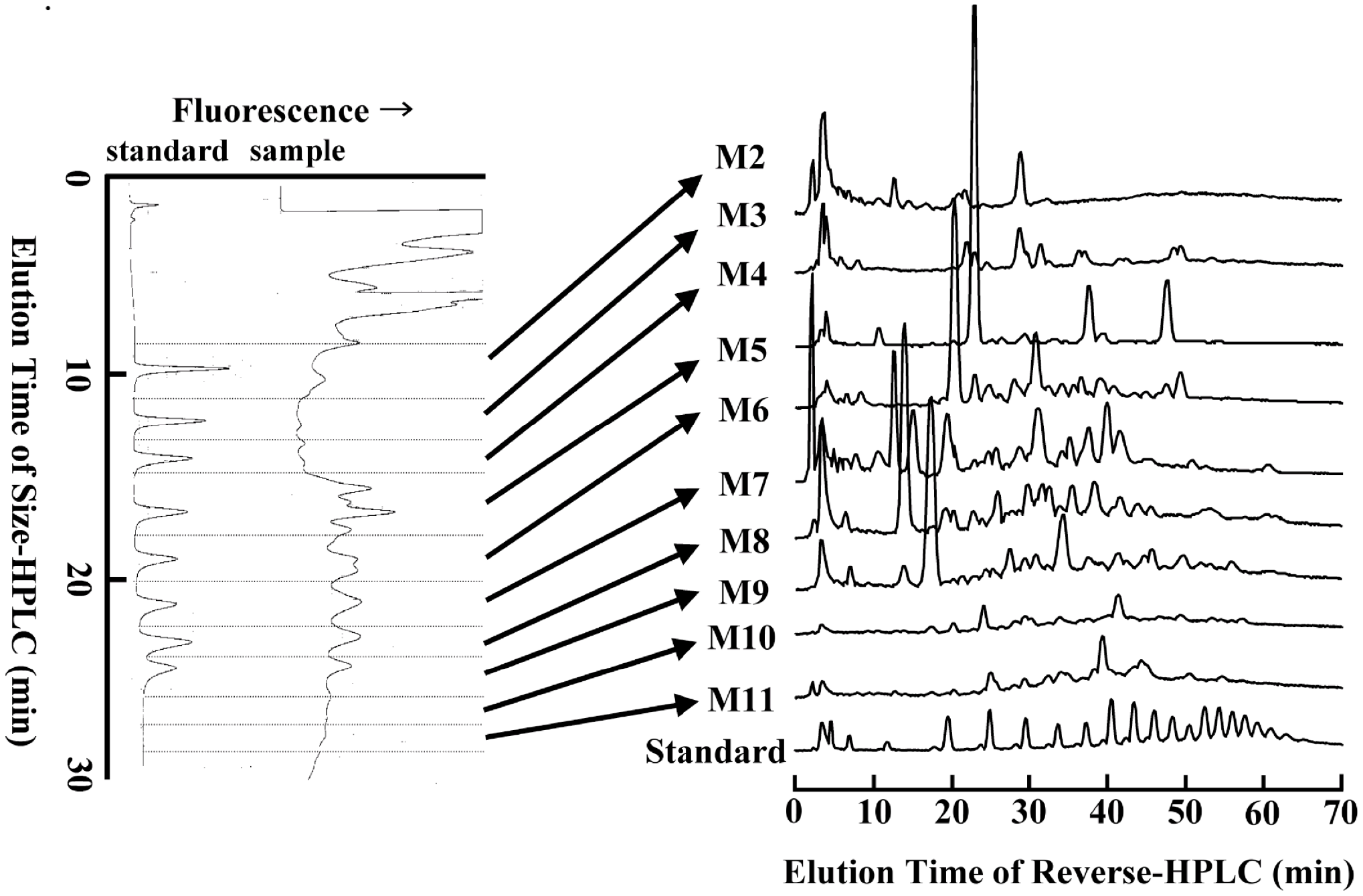
Fluorescence →
standard sample
0
10
20
30
Elution Time of Size-HPLC (min)
M2
M3
M4
M5
M6
M7
M8
M9
M10
M11
Standard
0
10
20
30
40
50
60
70
Elution Time of Reverse-HPLC (min)

Figure 5

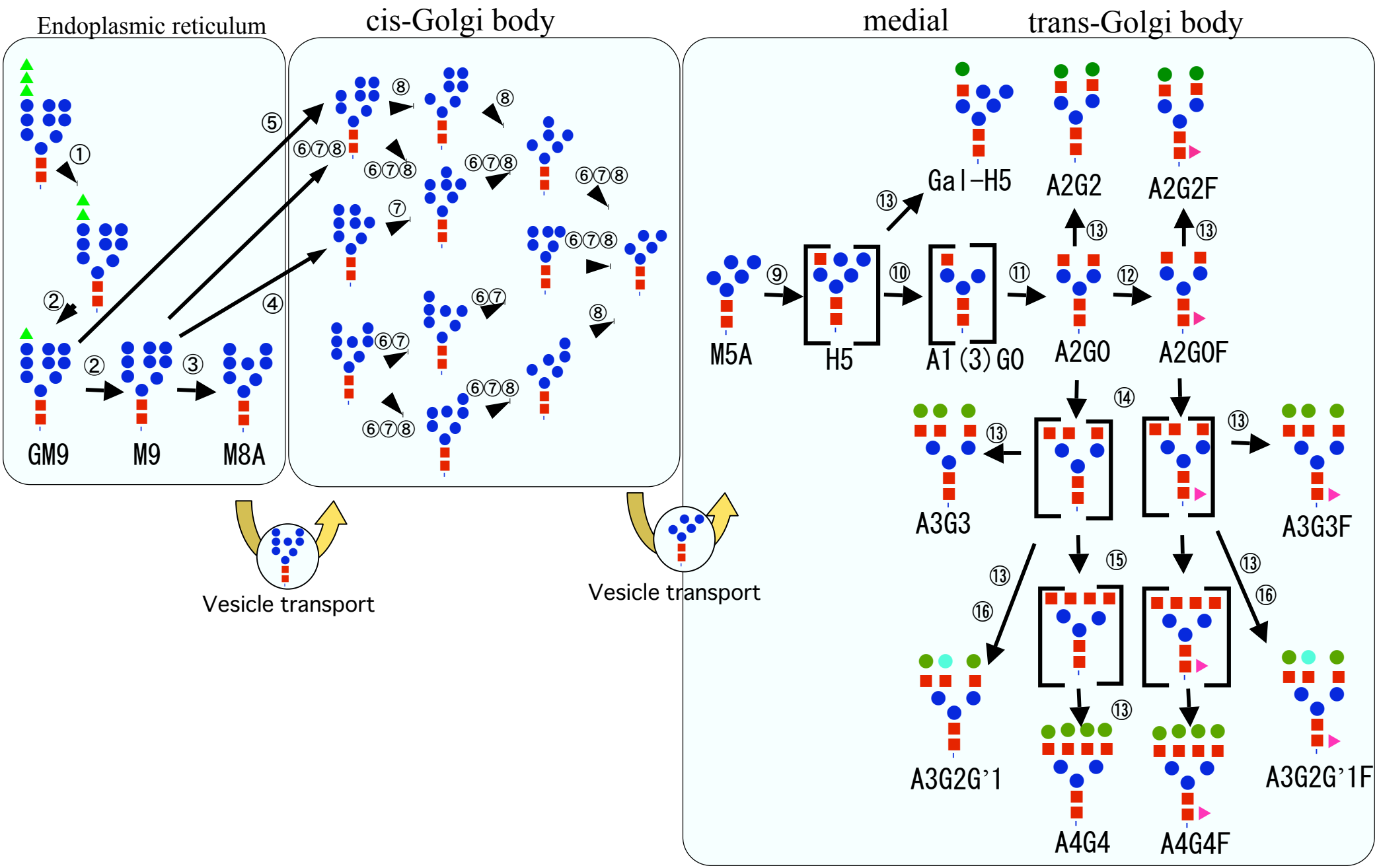
Endoplasmic reticulum
cis-Golgi body
medial
trans-Golgi body
GM9
M9
M8A
M5A
H5
A1(3)G0
A2G0
A2G0F
Gal-H5
A2G2
A2G2F
A3G3
A3G3F
A3G2G'1
A3G2G'1F
A4G4
A4G4F
Vesicle transport
Vesicle transport

Figure 6

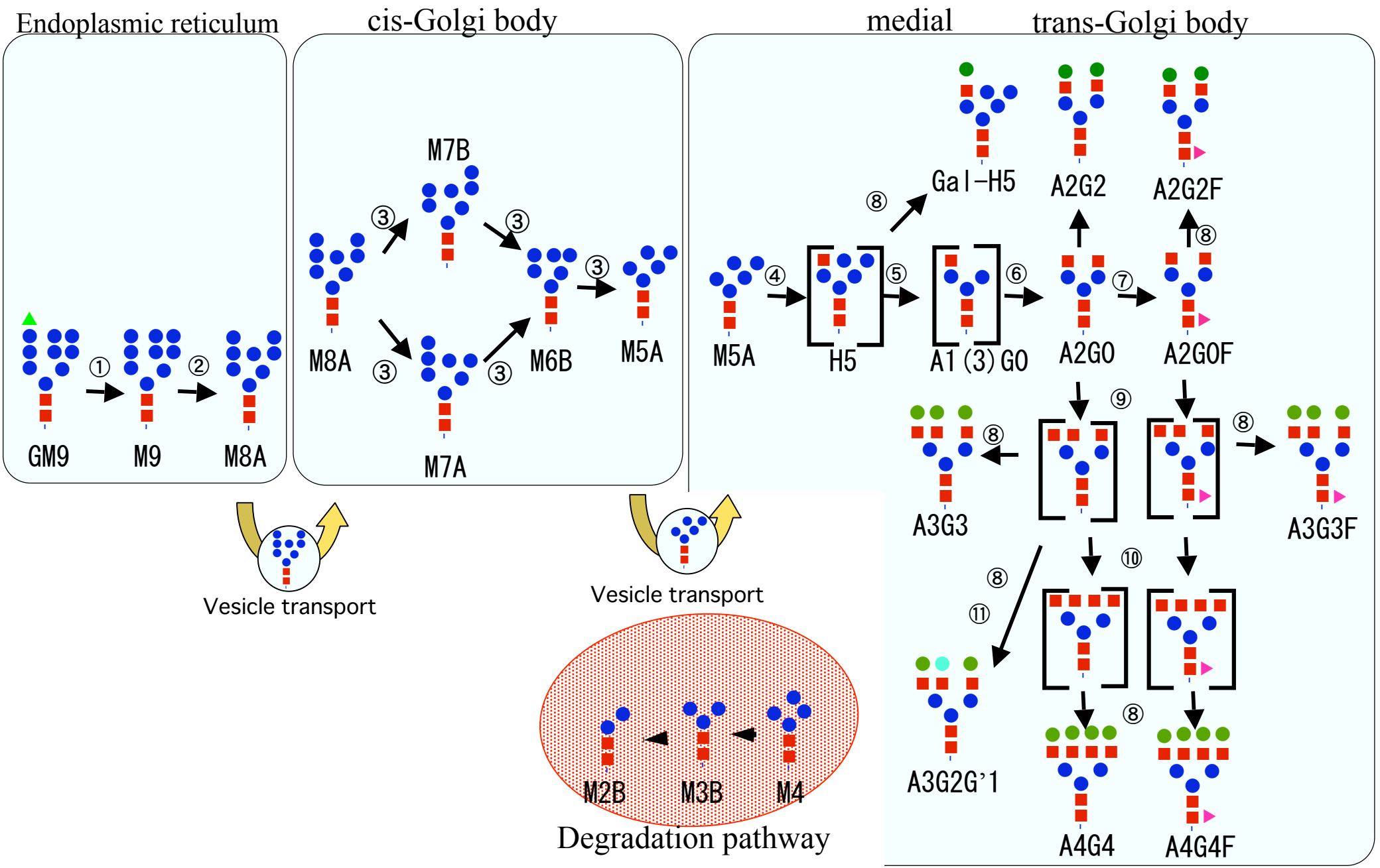
Endoplasmic reticulum
cis-Golgi body
medial
trans-Golgi body
GM9
M9
M8A
M7B
M8A
M6B
M5A
M7A
M5A
H5
Gal-H5
A1(3)G0
A2G2
A2G2F
A2G0
A2G0F
A3G3
A3G3F
A3G2G'1
A4G4
A4G4F
Vesicle transport
Vesicle transport
M2B
M3B
M4
Degradation pathway

Table1: The list of genes used in this study

		Gene name	Accession number
		Glucosidase	
	m	Glucosidase I	NM_020619
	m	Glucosidase II alpha subunit	NM_008060
	m	Acid α glucosidase	NM_008064
	m	Acid β glucosidase	NM_008094
		Mannnosidase	
	r	ER-mannosidase	M57547
	r	end-mannosidase	AF023657
	m	Golgi-mannosidase IA	NM_008548
	m	Golgi-mannosidase IB	NM_010763
	h	Golgi-mannosidase IC	AF261655
	m	Golgi-mannosidase II	NM_008549
	m	Golgi-mannosidase IIX	AF107018
	m	Lysosomal α-mannosidase	NM_010764
	m	Lysosomal β-mannosidase	NM_005908
	h	α 1,2-specific mannosidase	NM_016219
	m	MAN2B2	AB006458
	h	human(6A8) homolog	AF044414
		Acetylglucosaminyltransferase	
	m	1,3(i-β1,3GnT)	NM_006876
	m	1,6 (I-antigen)	NM_008105
	m	C2GnT1(C2GnT,C2GnT-L)	NM_010265
X	m	C2GnT2(C2/4GnT,GnT-M)	AB053217
	h	C2GnT3	NM_016591
	m	GnT I	NM_145926
	h	GnT I.2	NM_013244
	r	GnT II	U21662
	m	GnT III	L39373
	h	GnT 4A	NM_012214
	h	GnT 4B	NM_014275
	h	GnT 4H	NM_013244
	r	GnT V	L14284
X	c	GnT VI	AB040608
	m	GnT IX	AB119127
	m	LARGE	AJ006278
	r	O-GlcNAc transferase	U76557
X	m	α1,4 GnT	NM_016161
	m	β1,3GnT1	NM_016888
	h	β1,3GnT2	AB049584
	m	β1,3GnT3	AY037785
	m	β1,3GnT4	AY037786
	m	β1,3GnT5(Lc3synthase)	AY029203
X	h	β1,3GnT6	AB073740
X	m	β1,3GnT7	AF502429
	m	manic fringe	AF015769
	m	lunatic fringe	AF015768
	m	radical fringe	AF015770

c, m, r and h mean that sequence of the chick, mouse, rat or human gene were reported in the Gene Bank.
X indicates that sequence information of the genes was available, but their DNA could not be amplified.

Table1: The list of genes used in this study(continued)

		Gene name	Accession number
		Fucosyltransferase	
	m	Fuc-T I	NM_008051
	m	Fuc-T II	NM_018876
	m	Fuc-T IV	NM_010242
	m	Fuc-T VII	NM_013524
	m	Fuc-T VIII	NM_016893
	m	Fuc-T IX	NM_010243
X	m	Fuc-T X	NM_134161
	m	Fuc-T XI	XM_203633
	m	Sec1	NM_019934
	m	O-Fuc-T I	NM_080463
	m	O-Fuc-T II	BC018194
		Sialyltransferase	
	m	ST3Gal I	NM_009177
	m	ST3Gal II	NM_009179
	m	ST3Gal III	NM_009176
	m	ST3Gal IV	NM_009178
	m	ST3Gal V	NM_011375
	m	ST3Gal VI	AF119390
	m	ST6Gal I	NM_145933
	m	ST6GalNAc I	NM_011371
	m	ST6GalNAc II	NM_009180
	m	ST6GalNAc III	NM_011372
	m	ST6GalNAc IV	NM_011373
	m	ST6GalNAc V	NM_012028
	m	ST6GalNAc VI	NM_016973
	m	ST8Sia I	NM_011374
	m	ST8Sia II	NM_009181
	m	ST8Sia III	NM_009182
	m	ST8Sia IV	NM_009183
	m	ST8Sia V	NM_013666
	m	ST8Sia VI	NM_145838
		Galactosyltransferase	
	m	α1,3GT	NM_010283
	h	α1,4GT	AJ245581
	m	β1,3GT I	AF029790
	m	β1,3GT II	NM_020025
	m	β1,3GT III	AF029792
	m	β1,3GT IV	AF082504
	h	β1,3GT V	AF254738
	h	β1,3GT VI	NM_033149
	m	β1,3GT VIII	NM_080445
	m	β1,4GT I	J03880
	m	β1,4GT II	AF142670
	m	β1,4GT III	BC013619
	m	β1,4GT IV	AF142672
	m	β1,4GT V	NM_019835
	m	β1,4GT VI	NM_019737
	h	β1,4GT VII	NM_146045
X	m	ceramide GT	BC016885

c, m, r and h mean that sequence of the chick, mouse, rat or human gene were reported in the Gene Bank.
X indicates that sequence information of the genes was available, but their DNA could not be amplified.

Table1: The list of genes used in this study(continued)

		Gene name	Accession number
		Acetylgacetylalactosaminyltransferase	
	m	ABO blood group	NM_030718
X	m	CSGalNAcT1	XM_134236
X	m	CSGalNAcT2	NM_030165
	m	Galgt1 (GM2 synthase)	NM_008080
X	m	Galgt2 (CT antigen transferase)	NM_008081
	m	polypeptide GalNAcT1	NM_013814
	m	polypeptide GalNAcT2	AF348968
	m	polypeptide GalNAcT3	NM_015736
	m	polypeptide GalNAcT4	NM_015737
	r	polypeptide GalNAcT5	AF049344
	m	polypeptide GalNAcT6	AJ133523
	m	polypeptide GalNAcT7	AF349573
	r	polypeptide GalNAcT9	AF241241
X	m	polypeptide GalNAcT10	AK033515
X	m	polypeptide GalNAcT11	NM_144908
X	m	polypeptide GalNAcT12	NM_172693
X	m	polypeptide GalNAcT13	AB082928
X	m	polypeptide GalNAcT14	XM_128787
		EXT/EXTL	
	m	hereditary multiple exostoses 1	U78539
	h	hereditary multiple exostoses 2	U67837
	m	multiple exostoses-like 1	NM_019578
	m	multiple exostoses-like 2	NM_021388
	m	multiple exostoses-like 3	NM_018788
		Xylosyltransferase	
	m	XT I	AJ291750
	m	XT II	AJ291751
		Mannosyltransferase	
	m	O-MT I	NM_145145
	m	O-MT II	AY090482
		Sulfotransferase	
	m	HS2ST	NM_016922
	m	HS3ST1	AB040610
	h	HS3ST2	NM_033036
	h	HS3ST3A1	NM_024637
	m	HS3ST3B	NM_011828
	m	HS6ST1	NM_010474
	m	HS6ST2	NM_006043
	m	HS6ST3	NM_006042
X	m	GAL3ST1	NM_018805
X	h	GAL3ST2	NM_015818
X	h	GAL3ST3	NM_015819
X	h	GAL3ST4	NM_015820
	h	NDST1	NM_001543
	h	NDST2	XM_005875
	m	NDST3	NM_031186
	m	NDST4	NM_022565

c, m, r and h mean that sequence of the chick, mouse, rat or human gene were reported in the Gene Bank.
X indicates that sequence information of the genes was available, but their DNA could not be amplified.

Table 1: The list of genes used in this study(continued)

	Gene name	Accession number
	other	
m	GPA	AF187073
m	PLP	XM_136064
	House keeping gene	
m	β-actin	M12481
m	ubiquitin B	NM_011664
m	tyrosine 3-monooxygenase	NM_011740
m	stroma cell derived factor 4	NM_011341
m	ribosomal ptorein S29	NM_009093
m	myosin Ib	BC054786
m	glyceraldehyde-3-phosphate dehydrogenase	M32599
m	hypoxanthine guanine phosphoribosyl transferase	NM_013556

c, m, r and h mean that sequence of the chick, mouse, rat or human gene were reported in the Gene Bank. X indicates that sequence information of the genes was available, but their DNA could not be amplified.

Table 2: The results of gene expression analysis

Gene name	Gene expression level			
	E12 brain	Adult brain	kidney	liver
Glucosidase				
Glucosidase I	4.2	3.8	3.2	3.5
Glucosidase II alpha subunit	5.8	4.8	4.0	4.8
Acid α glucosidase	2.5	5.7	2.7	1.8
Acid β glucosidase	3.5	3.8	3.0	1.8
Mannnosidase				
ER-mannosidase	4.2	4.3	1.8	2.5
end-mannosidase	1.7	1.0	0.0	0.5
Golgi-mannosidase IA	1.5	3.5	4.3	6.3
Golgi-mannosidase IB	5.0	6.3	3.0	4.3
Golgi-mannosidase IC	1.0	3.0	0.3	0.0
Golgi-mannosidase II	1.0	1.7	1.2	4.3
Golgi-mannosidase IIX	0.0	0.0	0.0	0.0
Lysosomal α-mannosidase	2.0	2.0	3.5	1.8
Lysosomal β-mannosidase	0.0	0.7	1.5	0.5
α 1,2-specific mannosidase	4.8	6.3	5.2	4.8
MAN2B2	2.0	2.0	1.5	1.0
human(6A8) homolog	5.2	5.0	1.8	2.5
Acetylglucosaminyltransferase				
GnT I	3.0	3.0	3.8	3.0
GnT I.2	4.8	5.3	2.3	3.0
GnT II	4.5	4.3	4.3	4.3
GnT III	3.7	5.2	3.2	0.0
GnT 4A	0.7	3.2	0.8	0.0
GnT 4B	3.3	3.2	1.2	1.0
GnT 4H	0.0	0.0	0.3	0.0
GnT V	4.2	5.7	3.3	2.0
GnTIX	4.5	3.5	0.7	2.2
β1,3GnT1	3.0	5.2	4.5	3.0
β1,3GnT2	3.0	5.3	4.0	3.0
β1,3GnT3	0.0	0.0	0.0	0.0
β1,3GnT4	0.0	0.0	0.0	0.0
β1,3GnT5	5.0	0.8	0.0	0.0
manic fringe	5.7	1.5	1.0	1.0
lunatic fringe	3.7	2.0	0.0	0.0
radical fringe	4.3	5.2	1.5	2.5
LARGE	2.5	4.8	0.5	0.0
1,3(i-β1,3GnT)	1.0	3.3	2.0	1.5
1,6(I-antigen)	0.0	1.0	5.5	0.0
O-GlcNAc T	0.0	0.0	0.0	0.0
C2GnT1(C2GnT,C2GnT-L)	0.0	1.7	6.5	0.0
C2GnT3	1.5	2.0	0.0	0.0
Xylosyltransferase				
XT1	1.3	2.2	0.7	0.0
XT2	2.8	3.3	0.7	1.5
Mannosyltransferase				
o-MT1	2.7	2.0	0.3	1.5
o-MT2	1.8	2.0	0.5	1.3

The mRNA levels of glycosidases and glycosyltransferases were analyzed in four mouse tissue samples, 12-day fetal brain, 12-week postnatal brain, kidney and liver. The mRNA level of each gene was determined by comparing their intensities with those of the dilution series of GAPDH.

Table 2: The results of gene expression analysis

Gene name	Gene expression level			
	E12 brain	Adult brain	kidney	liver
Fucosyltransferase				
Fuc-T I	0.0	0.0	0.0	0.0
Fuc-T II	0.0	0.0	0.0	0.0
Fuc-T IV	0.0	0.0	0.0	0.0
Fuc-T VII	0.0	0.0	0.0	0.0
Fuc-T VIII	4.3	4.8	3.2	1.0
Fuc-T IX	1.5	4.8	4.0	0.0
Sec1	0.7	0.0	0.0	0.0
Fuc-T XI	6.0	5.5	0.0	1.5
O-Fuc-T I	2.7	2.3	0.8	1.3
O-Fuc-T II	0.0	0.0	0.0	0.0
Sialyltransferase				
ST3Gal I	0.7	0.7	0.7	3.5
ST3Gal II	4.8	5.7	0.8	0.0
ST3Gal III	3.3	4.3	2.8	4.0
ST3Gal IV	0.7	1.3	1.7	3.0
ST3Gal V	4.2	5.7	0.0	4.3
ST3Gal VI	1.7	2.0	2.3	0.0
ST6Gal I	3.3	1.7	0.3	3.5
ST6GalNAc I	0.0	1.0	0.3	0.0
ST6GalNAc II	0.0	1.0	3.5	0.0
ST6GalNAc III	1.3	1.3	0.0	0.0
ST6GalNAc IV	1.3	1.3	0.7	0.0
ST6GalNAc V	6.7	7.5	0.7	4.3
ST6GalNAc VI	3.0	6.0	0.0	2.3
ST8Sia I	1.3	1.0	1.2	0.0
ST8Sia II	5.8	1.0	0.5	0.0
ST8Sia III	2.7	3.8	0.0	0.0
ST8Sia IV	2.0	1.0	0.0	0.0
ST8Sia V	1.8	5.8	0.7	0.0
ST8Sia VI	0.0	0.0	0.0	0.0
Galactosyltransferase				
β1,3GT I	3.8	4.8	1.3	5.5
β1,3GT II	2.8	4.8	0.7	0.0
β1,3GT III	3.8	4.3	2.8	0.0
β1,3GT IV	1.3	1.3	0.0	0.0
β1,3GT V	1.3	2.0	1.3	0.0
β1,3GT VI	1.8	1.2	0.0	0.0
β1,3GT VIII	2.8	3.5	3.2	2.0
β1,4GT I	2.8	3.0	1.3	4.3
β1,4GT II	5.3	4.8	0.0	0.0
β1,4GT III	5.5	4.7	3.0	2.5
β1,4GT IV	2.2	2.0	0.3	0.0
β1,4GT V	3.8	4.7	5.8	3.3
β1,4GT VI	3.8	6.3	1.0	0.0
β1,4GT VII	1.8	0.3	0.3	0.0
α1,3GT	1.0	0.7	0.3	0.0
α1,4GT	4.8	4.2	5.7	7.0

The mRNA levels of glycosidases and glycosyltransferases were analyzed in four mouse tissue samples, 12-day fetal brain, 12-week postnatal brain, kidney and liver. The mRNA level of each gene was determined by comparing their intensities with those of the dilution series of GAPDH.

Table 2:The results of gene expression analysis

Gene name	Gene expression level			
	E12 brain	Adult brain	kidney	liver
Acetylgalactosaminyltransferase				
GalNAc T1	7.3	6.3	7.2	4.3
GalNAc T2	6.5	5.5	4.2	3.3
GalNAc T3	2.3	2.0	4.0	0.0
GalNAc T4	1.3	1.3	0.7	1.0
GalNAc T5	1.3	1.3	0.0	0.0
GalNAc T6	1.3	3.3	0.0	0.0
GalNAc T7	4.7	4.8	2.7	0.0
GalNAc T9	1.3	0.0	0.0	0.0
1,3(blood group A)	1.3	0.3	0.0	0.0
1,4(GM2 synthase)	4.8	6.2	1.8	5.8
EXT/EXTL	5.3	4.3	4.2	3.5
EXT1	5.0	4.8	3.8	3.5
EXT2	0.0	3.3	0.0	0.0
EXTL1	0.0	1.7	0.0	0.0
EXTL2	2.5	4.0	0.3	1.5
EXTL3				
Sulfotransferase				
HS2ST1	5.5	5.3	0.3	0.0
HS3ST1	3.3	5.3	0.0	0.5
HS3ST2	0.0	0.0	0.0	0.0
HS3ST3A	0.0	0.0	0.0	0.0
HS3ST3B	1.3	0.5	0.0	2.0
HS6ST1	4.8	3.5	5.3	5.8
HS6ST2	0.0	0.0	0.0	0.0
HS6ST3	1.5	2.8	0.0	0.0
NDST1	2.7	4.2	0.7	2.5
NSDT2	1.0	0.0	0.0	0.0
NDST3	2.3	4.8	0.0	0.0
NSDT4	1.3	3.8	0.0	0.0
GPG	1.3	1.3	0.3	2.0
PLP	5.7	10.0	3.0	4.0
House keeping				
stroma cell derived factor 4	6.5	6.8	5.0	6.0
myosine Ib	6.0	3.5	1.0	5.8
HGPT	5.3	6.5	4.3	5.8
ubiquitin B	12.0	11.7	11.0	10.0
tyrosine 3-monooxygenase	2.7	1.7	0.3	2.0
ribosomal protein S29	11.0	9.3	7.3	9.3
GAPDH	12.0	11.3	11.0	11.3
β-actin	12.0	10.3	7.3	9.5

The mRNA levels of glycosidases and glycosyltransferases were analyzed in four mouse tissue samples, 12-day fetal brain, 12-week postnatal brain, kidney and liver. The mRNA level of each gene was determined by comparing their intensities with those of the dilution series of GAPDH.

Table 3: Primer Pairs and PCR Conditions

Clone name	Primer sequences	Expected size (bp)	PCRcycle
GnT III	5'-CCTCAAACTCTACGATGGCT-3' 5'-CTACCCAGCCCTGTGAAAGTGCACA-3'	649	30
2,8-ST V	5'-ATGCGCTACGCAGACCCCT-3' 5'-TCAGCAGCAATTGCAGGTGC-3'	1241	30
Man IB	5'-GTAGGATACCACCTTTGAAC-3' 5'-ACCAACTGATGTGTGATACT-3'	1153	30
β1,3GT I	5'-ATGGCTTCAAAGGTCTCCTG-3' 5'-CTAACATCTCAGATGCTTCTTGCTT-3'	983	35
Fuc-T VIII	5'-CTATACTACCTCAGTCAAAC-3' 5'-TATTTGACAAACTGGGACAC-3'	505	30
Fuc-T IX	5'-ACAACAAATCCCATGCGGTC-3' 5'-GTGGGAATCAGATTTTTATC-3'	405	30
GAPDH	5'-ATGGTGAAGGTCGGTGTGAACGGA-3' 5'-TTACTCCTTGGAGGCCATGTAGGC-3'	1004	25

GnTIII, N-acetylglucosaminyltransferase III; 2,8-ST V, 2,8-sialyltransferase V; ManIB, Golgi-mannosidase IB; b1,3GT I, b1,3-galactosyltransferase 1; Fuc-T VIII, fucosyltransferase VIII; Fuc-T IX, fucosyltransferase IX; GAPDH, glyceraldehyde-3-phosphate dehydrogenase.

Note. Template cDNAs for RT-PCR were synthesized from 200ng of poly(A)+ RNAs using 200 U Superscipt II reverse and random(N6) primers. PCRs were carried out using 0.25U Taq DNApolymerase, 200 mM dNTP, 2 mM each primer sets, and the template cDNAs. PCR conditions were as follows; after incubation for 5 min at 96 ˚C, 25-35 cycles of denaturing at 96 ˚C for 45 s, annealing at 60 ˚C for 45 s, extention at 72 ˚C for 90s, and then final extention at 72 ˚C for 7min.

Table 4: Structures of desialylated sugar chains derived from several tissues

Structure	Tissue			
	12-day embryo brain	Adult brain	Kidney	Liver
	%	%	%	%
GM9	1.9	0.4	4.1	5.2
M9A	10.2	4.7	8.4	13.9
M8A	11.2	5.2	5.1	14.7
M7A	3.8	2.0	1.9	3.0
M7B	2.6	2.5	2.1	2.5
M6B	9.9	7.6	6.0	7.6
M5A	7.6	23.5	5.7	5.9
M4	1.3	0.5	1.0	1.2
M3B	0.7	0.3	1.1	1.7
M2B	0.2	0.2	2.2	5.9
A0G0F	0.9	1.5	2.6	0.0
A1(6)G0F	0.0	0.3	0.3	0.0
A2G0	0.0	0.0	0.0	1.2
A2G0B	0.4	0.9	0.4	0.0
A2G2	1.9	4.4	1.4	12.7
A2G2F	4.1	1.1	3.7	2.7
A2G1Fo(6)FB	1.0	2.2	0.0	0.0
A2G'2F	0.0	0.8	0.0	0.0
A2G1Fo(6)G'1(3)F	0.0	0.6	0.0	0.0
A2G2FB	4.9	0.1	0.0	0.0
A2G1Fo(3)FB	0.4	1.5	0.0	0.0
A2G2Fo2FB	0.8	1.2	0.0	0.0
LewsX2-BA-2	0.0	0.0	12.9	0.0
LewisXa-BA-2	0.0	0.0	2.5	0.0
Ga+GbBA-2	2.2	0.7	0.0	0.0
G2-BA-2	0.0	0.0	0.5	0.0
BA1(A1(6)G0FB)	0.3	4.2	0.4	0.0
BA2(A2G0FB)	1.8	4.3	0.6	0.0
H5B	0.0	0.0	0.7	0.0
H5.1	0.4	0.6	0.0	0.0
LewisX-H4	0.0	0.0	2.1	0.0
LewisX-H4FB	1.3	1.3	0.0	0.0
High mannose type	47.3	45.8	33.2	52.7
Oligo mannose type	2.2	1.0	4.2	8.8
complex type	18.5	23.8	25.2	16.5
core fucose addition	17.5	19.8	23.4	2.7
Bisecting GlcNAc addition	13.0	16.4	17.3	0.0
Lewis X structure	2.4	4.6	17.5	0.0
Lewis X structure*2	4.2	8.0	30.3	0.0
Hybrid type	1.7	2.0	2.8	0.0
Other structure	30.3	27.5	34.7	22.0
Total	100.0	100.0	100.0	100.0

(a)The value is expressed as the percentage of sugar chains containing the indicated struccture in the total of N-linked sugar chains.
(b)The value is expressed as a total of high mannose-type sugar chains(mannose residues=5-9)
(c)The value is expressed as a total of the percentage of N-linked sugar chains containing oligomannose(mannose residues=2-4)
(d) The value is expressed as a total of other forms sugar chains which structures were not determined.

Major N-linked sugar chains expressed in mouse tissue. The nomenclature of the sugar chains is shown in “Abbreviations” and Table 5. The values shown are the relative abundances (RA) against total N-linked sugar chains from M2 to M11 fraction.

Table 5: Structures and abbreviations of PA-sugar chains.

Abbreviation	structure
GM9	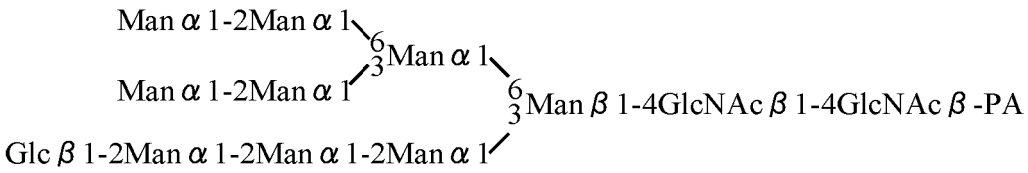
M9A	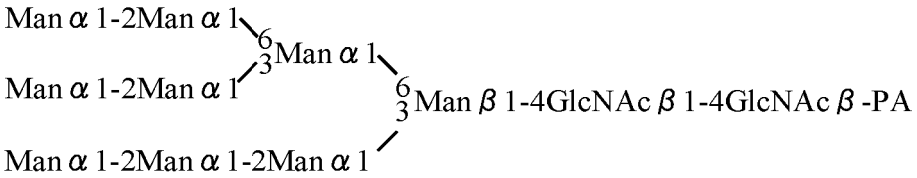
M8A	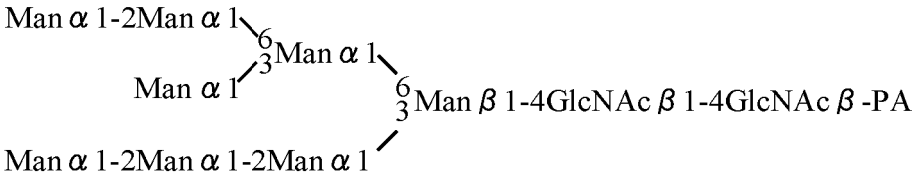
M7A	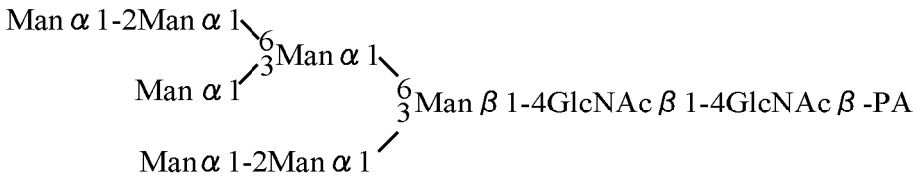
M7B	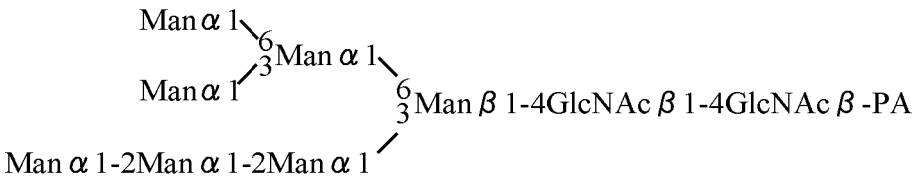
M6B	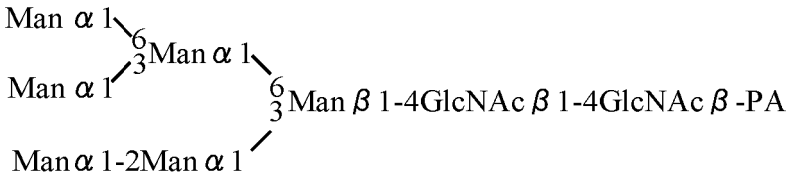
M5A	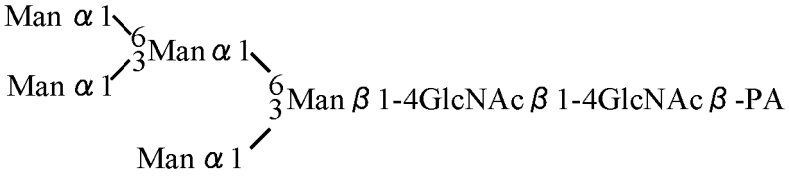
M4B	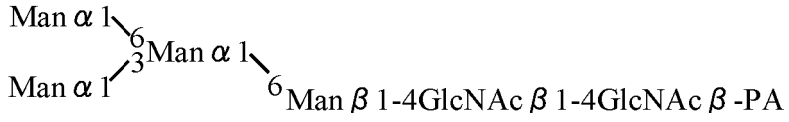

Table 5: Structures and abbreviations of PA-sugar chains(continue).

Abbreviation	structure
M3B	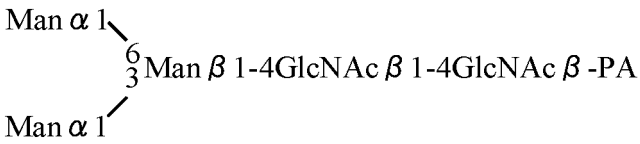
M2B	
A0G0F	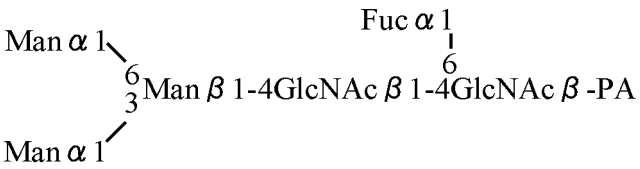
A1(6)G0F	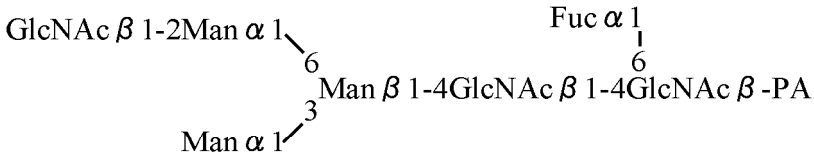
A2G0	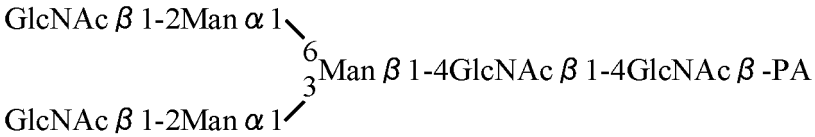
A2G0B	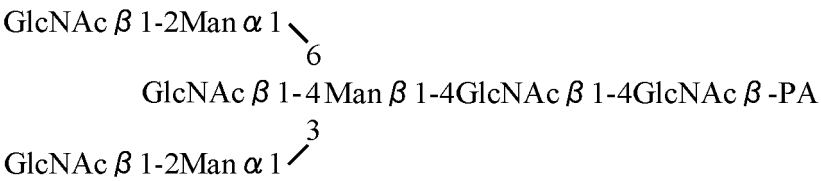
A2G2	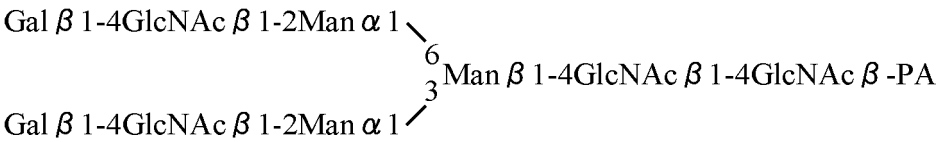
A2G2F	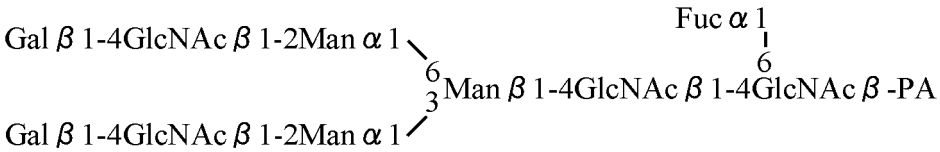

Table 5: Structures and abbreviations of PA-sugar chains(continue).

Abbreviation	structure
A2G1Fo(6)FB	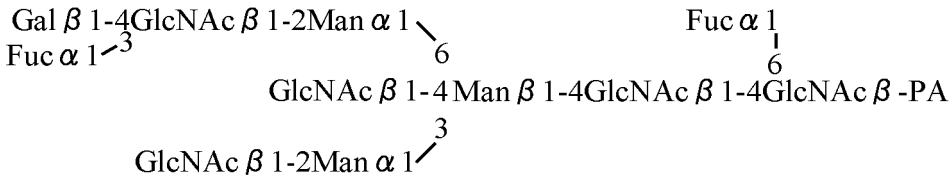
A2G'2F	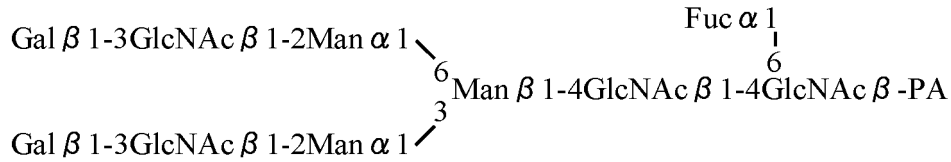
A2G1Fo(6)G'1(3)F	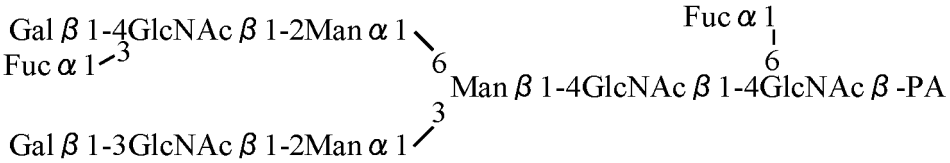
A2G2FB	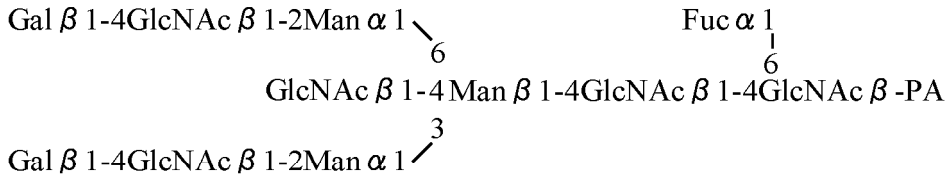
A2G1Fo(3)FB	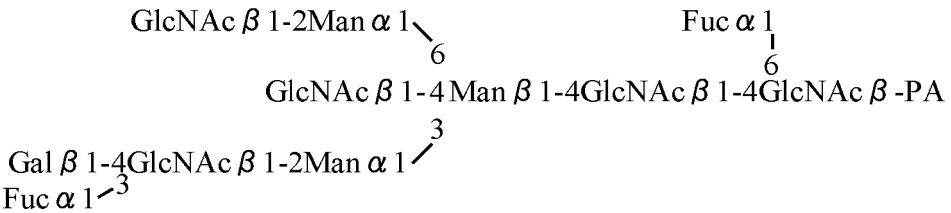
A2G2Fo2FB	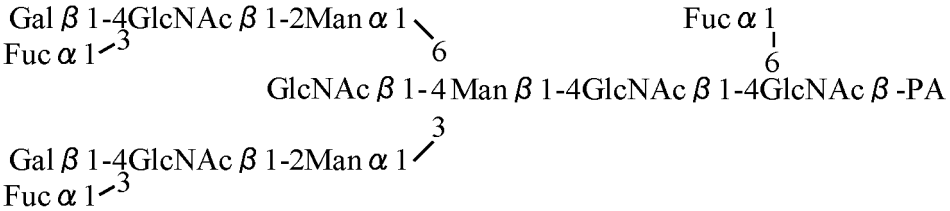
LewisX2-BA-2	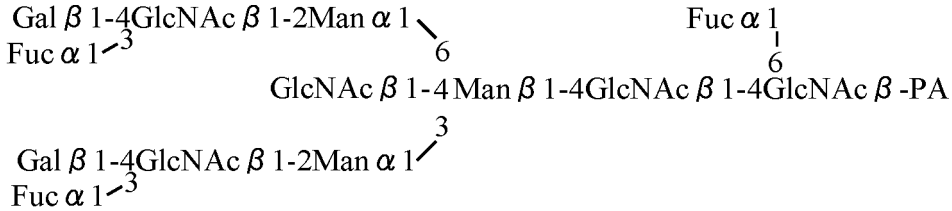
LewisXa-BA-2	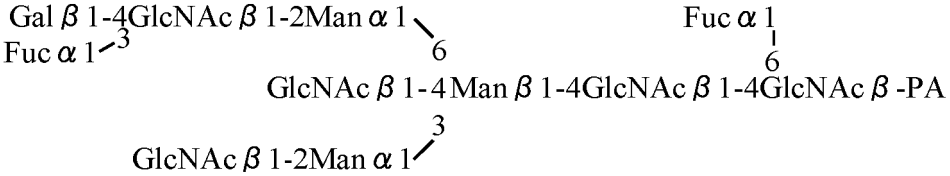

Table 5: Structures and abbreviations of PA-sugar chains(continue).

Abbreviation	structure
GaBA2	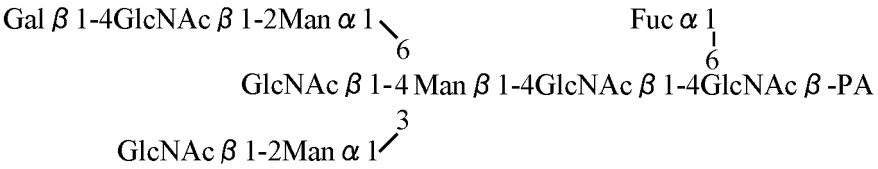
GbBA2	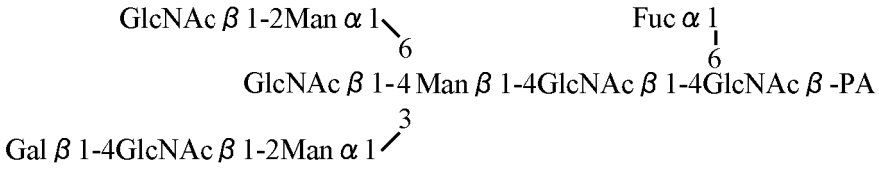
G2-BA2	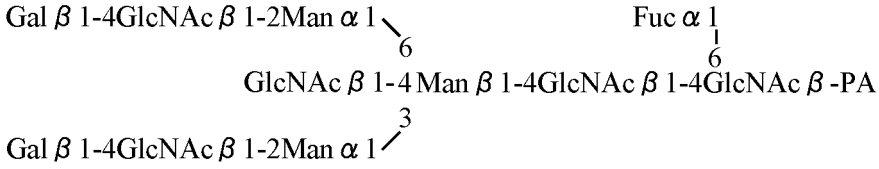
BA1	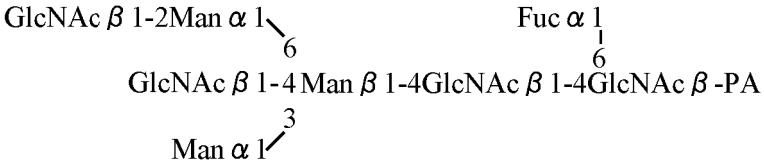
BA2	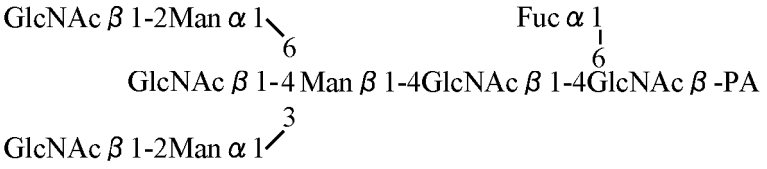
H5B	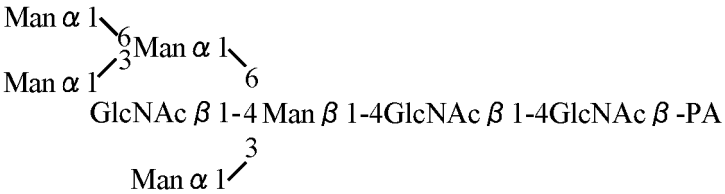
H5.1	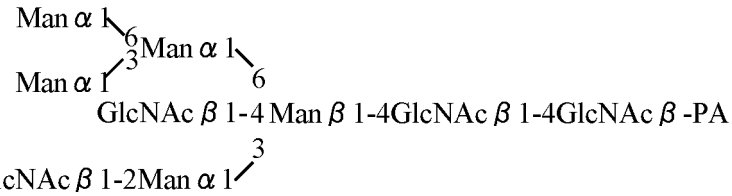
LewisX-H4	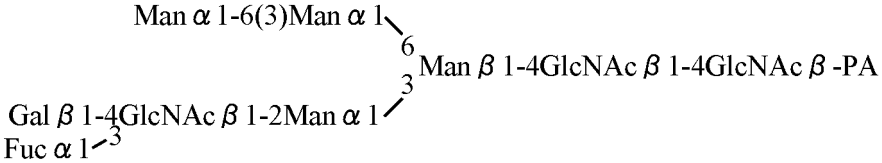
LewisX-4FB	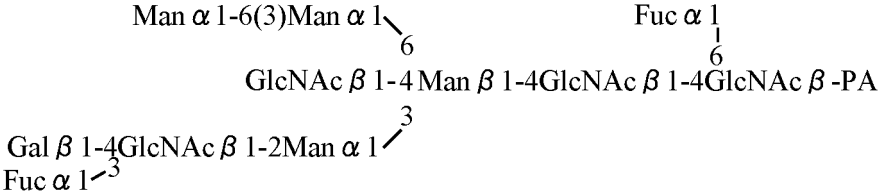

Table 5: Structures and abbreviations of PA-sugar chains(continue).

Abbreviation	structure
A3G3	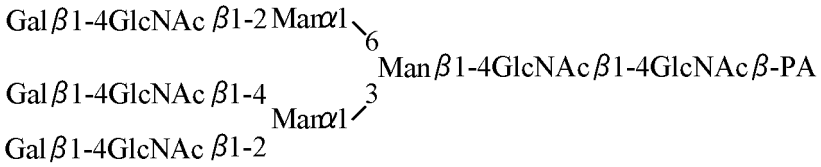
A3G3F	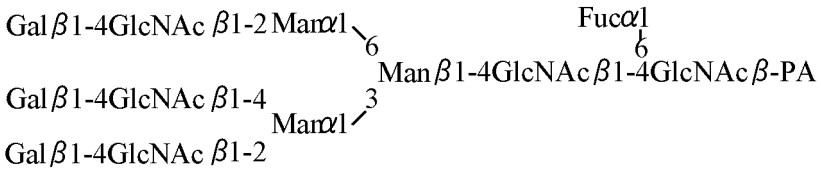
A3G2G'1(4)	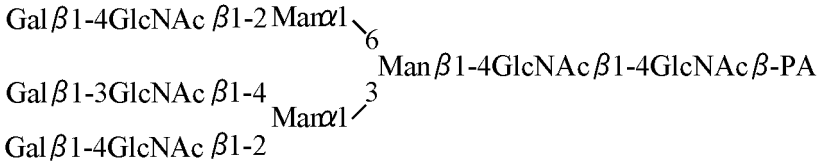
A4G4	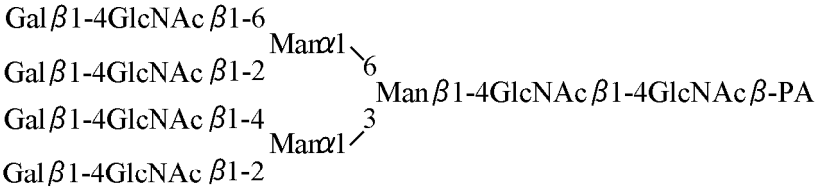
A4G4F	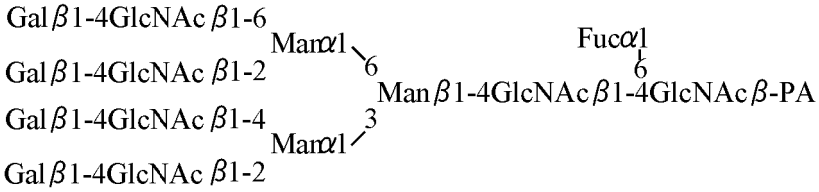
Gal-H5	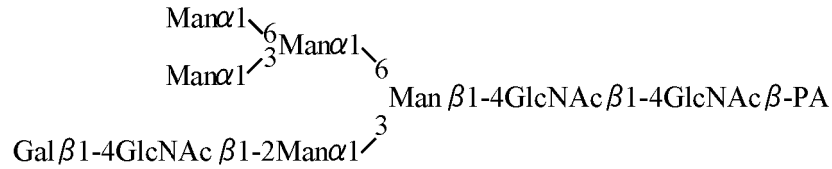

Table6. Structures of desialylated N-linked sugar chains derived from cell lines and adult liver.

sugar chain	cell lines						
	Neuro2a	N1E115	NB41A	C8D1A	C8D30	C8S	Liver
	%	%	%	%	%	%	%
GM9	3.2	1.2	2.6	1.9	1.2	1.3	5.2
M9A	8.9	4.7	10.5	6.6	5.3	7.0	13.9
M8A	7.0	7.8	11.2	4.6	4.7	5.5	14.7
M7A	3.7	3.3	3.3	2.5	2.4	3.2	3.0
M7B	2.4	3.0	2.6	1.8	1.7	1.9	2.5
M6B	8.9	11.0	8.3	4.7	6.1	11.2	7.6
M5A	2.4	4.0	3.5	3.3	2.5	3.9	5.9
M4	0.7	0.6	0.5	1.9	2.4	1.2	1.2
M3B	1.2	1.4	0.9	3.3	4.8	1.7	1.7
M2B	3.7	3.6	3.4	21.5	30.1	4.3	5.9
oligo mannose type	5.6	4.8	5.6	26.7	37.3	7.1	8.8
high mannose type	36.6	41.9	35.0	25.3	23.9	34.0	52.7
total M9+M8	15.9	12.5	21.7	11.1	9.9	12.4	28.6
total M8+M7	13.1	14.1	17.0	8.9	8.8	10.6	20.2
total M7+M6	15.0	17.3	14.1	9.1	10.2	16.3	13.1
total M4+M3+M2	5.6	5.6	4.8	26.7	37.3	7.1	8.8
A0G0F	0.0	1.6	1.0	1.6	1.4	2.0	0.0
A2G0	4.5	12.0	11.0	2.2	2.5	3.7	1.2
A2G2	10.9	9.8	2.7	2.4	2.7	2.8	12.7
A2G2F	0.5	6.0	4.5	3.7	2.9	7.8	2.7
A2G0F	0.0	1.6	0.0	0.0	0.0	0.0	0.0
A3G2G'1(4)	0.9	0.0	0.5	0.6	0.5	0.6	0.0
A3G3	2.4	0.0	2.3	3.4	3.3	1.1	0.0
A3G3F	0.1	0.0	0.2	2.1	1.1	1.9	0.0
A4G4	1.8	0.0	0.0	0.0	0.0	0.0	0.0
A4G4F	0.0	0.0	1.1	1.8	0.9	0.0	0.0
Gal-H5	1.6	0.5	0.0	0.9	0.4	1.7	0.0
total core fucose addition	0.6	6.7	9.2	9.3	6.3	11.7	2.7
total complex type	21.2	31.0	23.3	17.9	15.3	20.0	16.5
total hybrid type	1.6	0.0	0.5	0.9	0.4	1.7	0.0

N-linked sugar chains expressed in 6 cell lines and adult liver. The nomenclature of the sugar chains is shown in "Abbreviations" and Table 5. The values shown are the relative abundances (RA) against total N-linked sugar chains from M2 to M11 fraction.

Table7. The gene expression analysis of 6 cell lines and adult liver.

Gene name	cell lines						
	Neuro2a	N1E115	NB41A	C8D1A	C8D30	C8S	Liver
GnT I	3.8	2.5	4.0	3.0	2.8	5.2	3.0
GnT II	4.2	4.0	4.7	4.5	4.2	7.0	4.3
GnT III	2.3	2.5	4.5	1.5	0.0	4.2	0.0
GnT 4A	1.0	2.5	1.2	1.0	0.7	1.2	0.0
GnT 4B	2.3	2.5	1.3	1.5	4.5	6.2	1.0
GnT 4H	0.0	2.5	1.3	0.0	0.7	0.0	0.0
GnT V	4.0	4.0	3.3	3.8	2.7	2.0	2.0
GnT IX	0.0	0.0	1.7	1.0	3.0	6.0	2.2
β1,3GT I	2.3	4.5	2.5	3.0	0.0	7.0	0.0
β1,3GT III	2.8	1.5	4.8	3.5	3.0	1.3	0.0
β1,3GT V	2.5	4.8	2.5	3.0	1.5	3.2	0.0
β1,3GT VIII	1.2	5.2	3.0	3.5	3.8	3.5	2.0
β1,4GT I	4.0	3.0	3.2	3.8	3.8	5.8	4.3
β1,4GT II	2.5	3.3	5.3	3.3	3.5	6.2	0.0
β1,4GT III	4.7	3.5	4.3	3.8	4.0	4.8	2.5
β1,4GT IV	1.2	2.8	1.3	1.0	0.0	1.7	0.0
β1,4GT V	4.5	3.3	6.7	3.0	3.0	1.7	3.3
glucosidase I	5.7	4.5	6.3	3.5	5.3	5.2	3.5
glucosidase II	6.3	4.8	6.8	5.5	6.5	6.7	4.8
acid α-glucosidase	6.8	4.5	6.5	5.5	4.5	5.3	1.8
acid β-glucosidase	5.5	3.3	5.2	5.5	5.0	5.5	1.8
Fuc-T IV	1.0	1.3	0.0	0.5	0.0	0.0	0.0
Fuc-T VII	1.0	1.3	0.0	0.8	0.0	0.0	0.0
Fuc-T VIII	2.5	2.5	4.8	4.3	2.0	3.5	0.0
Fuc-T IX	2.3	2.5	1.5	0.8	2.0	2.0	0.0
Fuc-T X	0.0	1.3	0.0	0.8	2.0	0.0	0.0
Fuc-T XI	0.0	0.0	1.7	1.0	2.5	3.2	1.5
ER-Mannosidase	4.3	2.5	5.2	1.0	3.0	5.3	2.5
end-Mannosidase	0.0	0.0	0.0	1.0	2.0	1.3	0.5
Golgi-Mannosidase IA	0.0	0.0	0.0	0.5	0.0	1.2	6.3
Golgi-Mannosidase IB	6.2	4.5	7.0	5.0	5.5	6.0	4.3
Golgi-Mannosidase IC	2.2	3.0	1.8	1.0	3.0	3.7	0.0
Mannosidase II	1.2	3.5	1.8	1.0	3.0	1.3	4.3
Lysomal α–Mannosidase	4.5	3.5	5.5	3.8	4.0	5.8	1.8
Lysomal β-Mannosidase	3.5	3.0	0.0	3.8	4.5	3.0	0.5
MAN2B2	6.2	4.5	6.7	5.8	6.5	9.2	4.8
human(6A8) homolog	1.7	1.5	1.3	1.0	0.0	3.8	1.0
h α1,2-specific	4.7	3.0	3.7	3.8	4.0	5.8	2.5

The gene expressions of glyco-related gene were analyzed in six mouse cell lines(Neuro2a, NB41A, N1E115, C8D1A, C8D30, C8S) and adult liver.

Table8 :The correlation between N-linked sugar chins and gene expression.

	GM9
M9A	0.94
Total M9+M8	0.91
Lysosomal α-mannosidase	-0.81
glucosidase II	-0.70

	M9A
GM9	0.94
M8A	0.87
Total M9+M8	0.96
Total M8+M7	0.83
glucosidase II	-0.81
acid β-glucosidase	-0.86

	M8A
GM9	0.82
M9A	0.87
Total M9+M8	0.97
Total M8+M7	0.98
high mannose type	0.85
acid β-glucosidase	-0.94

	M7A
Total M7+M6	0.84
oligo mannose type	-0.89
M4	-0.90
M3B	-0.87
M2B	-0.89

	M7B
M4	-0.82
Lysosomal β-mannosidase	-0.81
complex	0.82

	M6B
Total M7+M6	0.98
ER-Mannosidase	0.92

	M5A
high mannose type	0.81

	M4
M7B	-0.82
M7A	-0.90
Total M7+M6	-0.82
M3B	0.97
M2B	0.95
oligo mannose type	0.96

	M3B
M7A	-0.87
M4	0.97
M2B	0.98
oligo mannose type	0.98

	M2B
M7A	-0.89
Total M7+M6	-0.86
M4	0.95
M3B	0.98
oligo mannose type	1.00

	oligo mannose type
M7A	-0.89
Total M7+M6	-0.86
M4	0.96
M3B	0.98
M2B	1.00

	high mannose type
M8A	0.85
Total M8+M7	0.89
M5A	0.81
A2G2	0.83
Lysosomal β–mannosidase	-0.86

	Total M9+M8
GM9	0.91
M9A	0.96
M8A	0.97
Total M8+M7	0.94
acid β-glucosidase	-0.93

	Total M8+M7
M9A	0.83
M8A	0.98
Total M9+M8	0.94
high mannose type	0.89

	Total M7+M6
M7A	0.84
M6B	0.98
M4	-0.82
M2B	-0.86
oligo mannose type	-0.86
ER-Mannosidase	0.87

Correlation coefficient between relative amount of each N-glycan and the relative amounts of each glyco-related gene mRNA was calculated.
A cutoff value for the significance was tentatively configulated to 0.8. Red character shows the gene, blue character shows the sugar chain.

Table 8:The correlation between N-linked sugar chins and gene expression

Oligo mannose type	
M7A	-0.89
Total M7+M6	-0.85
M4	0.96
M3B	0.99
M2B	1.00

A2G2	
high mannose type	0.83
A2G2	0.84

hybrid type	
Gal-H5	0.91

GnT I	
MAN2B2	0.89
ER-Mannosidase	0.82
6A8	0.83
h α1,2-specific	0.82
GnT II	0.87

β1,4GT III	
glucosidase II	0.85
acid-glucosidase a	0.87
h α1,2-specific	0.89
Golgi-mannosidase IB	0.81
mannosidase II	-0.80
Lysosomal α–mannosidase	0.94

mannosidase II	
acid α-glucosidase	-0.85
acid β-glucosidase	-0.91
β1,4GT III	-0.80
Gal-H5	-0.84

A0G0F	
GM9	-0.89

A2G2F	
core fucose	0.84

core fucose	
A2G2F	0.84
A2G2	-0.82

GnT II	
MAN2B2	0.89
GnT I	0.87

ER-Mannosidase	
M6B	0.92
Total M7+M6	0.87
glucosidase I	0.84
Golgi-mannosidase IB	0.80
GnT I	0.82

glucosidase I	
glucosidase II	0.82
ER-Mannosidase	0.84
Golgi-mannosidase IB	0.89

A2G0	
complex type	0.90

Gal-H5	
hybrid type	0.91
mannosidase II	-0.84

complex type	
A2G0	0.85
M7B	0.82

GnT III	
β1,4GT II	0.80

Golgi-mannosidase IB	
glucosidase II	0.92
glucosidase I	0.89
ER-Mannosidase	0.80
Lysosomal α–mannosidase	0.86
β1,4GT III	0.81

glucosidase II	
GM9	-0.70
M9A	-0.81
M8A	-0.72
glucosidase I	0.82
ER-Mannosidase	0.74
Golgi-mannosidase IB	0.92
β1,4GT III	0.85

Correlation coefficient between relative amount of each N-glycan and the relative amounts of each glyco-related gene mRNA was calculated. A cutoff value for the significance was tentatively configulated to 0.8. Red character shows the gene, blue character shows the sugar chain.

Table 8:The correlation between N-linked sugar chins and gene expression

acid α-glucosidase	
acid β-glucosidase	0.88
β1,4GT III	0.87

acid β-glucosidase	
M9A	-0.86
M8A	-0.94
Total M9+M8	-0.93
acid α-glucosidase	0.88
glucosidase II	0.81
mannosidase II	-0.91
β1,4GT III	0.89

Lysosomal mannosidase a	
GM9	-0.81
glucosidase II	0.86
acid α-glucosidase	0.81
acid β-glucosidase	0.83
MAN2B2	0.82
Golgi-mannosidase IB	0.86
h α1,2-specific	0.81
β1,4GT III	0.94

h α1,2-specific	
MAN2B2	0.91
Lysosomal α–mannosidase	0.81
GnT I	0.82
β1,4GT III	0.89

Lysosomal β–mannosidase	
M7B	-0.81
high mannose type	-0.86

MAN2B2	
glucosidase II	0.80
h α1,2-specific	0.91
Lysosomal α–mannosidase	0.82
GnT I	0.89
GnT II	0.89

6A8	
GnT I	0.83

Correlation coefficient between relative amount of each N-glycan and the relative amounts of each glyco-related gene mRNA was calculated. A cutoff value for the significance was tentatively configulated to 0.8. Red character shows the gene, blue character shows the sugar chain.